

Accepted Manuscript

Coumarin- dithiocarbamate hybrids as novel multitarget AChE and MAO-B inhibitors against Alzheimer's Disease: Design, synthesis and biological evaluation

Qi He, Jing Liu, Jin-Shuai Lan, Jiaoli Ding, Yongbing Sun, Yuanying Fang, Neng Jiang, Zunhua Yang, Liyuan Sun, Yi Jin, Sai-Sai Xie

PII: S0045-2068(18)30840-X
DOI: <https://doi.org/10.1016/j.bioorg.2018.09.010>
Reference: YBIOO 2507

To appear in: *Bioorganic Chemistry*

Received Date: 7 August 2018
Revised Date: 5 September 2018
Accepted Date: 7 September 2018

Please cite this article as: Q. He, J. Liu, J-S. Lan, J. Ding, Y. Sun, Y. Fang, N. Jiang, Z. Yang, L. Sun, Y. Jin, S-S. Xie, Coumarin- dithiocarbamate hybrids as novel multitarget AChE and MAO-B inhibitors against Alzheimer's Disease: Design, synthesis and biological evaluation, *Bioorganic Chemistry* (2018), doi: <https://doi.org/10.1016/j.bioorg.2018.09.010>

This is a PDF file of an unedited manuscript that has been accepted for publication. As a service to our customers we are providing this early version of the manuscript. The manuscript will undergo copyediting, typesetting, and review of the resulting proof before it is published in its final form. Please note that during the production process errors may be discovered which could affect the content, and all legal disclaimers that apply to the journal pertain.



**Coumarin- dithiocarbamate hybrids as novel multitarget AChE and MAO-B
inhibitors against Alzheimer's Disease: Design, synthesis and biological
evaluation**

Qi He,^{‡a} Jing Liu^{‡b}, Jin-Shuai Lan^c, Jiaoli Ding^a, Yongbing Sun^a, Yuanying Fang^a,
Neng Jiang^d, Zunhua Yang^b, Liyuan Sun^e, Yi Jin^{*a}, Sai-Sai Xie^{*a}

^aNational Pharmaceutical Engineering Center for Solid Preparation in Chinese Herbal Medicine, Jiangxi University of Traditional Chinese Medicine, Nanchang 330006, PR China

^bSchool of Pharmacy, Jiangxi University of Traditional Chinese Medicine, Nanchang 330006, PR China

^cExperiment Center of Teaching & Learning, Shanghai University of Traditional Chinese Medicine, Shanghai 201203, PR China

^dDepartment of Pharmacy, Affiliated Tumor Hospital of Guangxi Medical University, Nanning 530021, Guangxi, PR China

^eGuangxi Key Laboratory of Brain and Cognitive Neuroscience, Guilin Medical University, Guilin 541004, PR China

* Corresponding Author. E-mail: jinyixsnc@126.com (Y. Jin);
xiesaisainanchang@hotmail.com (S.-S. Xie);

[‡] These authors contributed equally.

Abstract

A series of new coumarin-dithiocarbamate hybrids were designed and synthesized as multitarget agents for the treatment of Alzheimer's disease. Most of them showed potent and clearly selective inhibition towards AChE and MAO-B. Among these compounds, compound **8f** demonstrated the most potent inhibition to AChE with IC₅₀ values of 0.0068 μ M and 0.0089 μ M for eeAChE and hAChE, respectively. Compound **8g** was identified as the most potent inhibitor to hMAO-B, and it is also a good and balanced inhibitor to both hAChE and hMAO-B (0.114 μ M for hAChE; 0.101 μ M for hMAO-B). Kinetic and molecular modeling studies revealed that **8g** was a dual binding site inhibitor for AChE and a competitive inhibitor for MAO-B. Further studies indicated that **8g** could penetrate the BBB and exhibit no toxicity on SH-SY5Y neuroblastoma cells. More importantly, **8g** did not display any acute toxicity in mice at doses up to 2500 mg/kg and could reverse the cognitive dysfunction of scopolamine-induced AD mice. Overall, these results highlighted **8g** as a potential multitarget agent for AD treatment and offered a starting point for design of new multitarget AChE/MAO-B inhibitors based on dithiocarbamate scaffold.

Keywords: Coumarin, dithiocarbamate, cholinesterase, monoamine oxidase, Alzheimer's disease.

1. Introduction

Alzheimer's disease (AD) is one of the most disastrous neurodegenerative diseases characterized by memory loss, degradation in language skills, behavioral abnormalities and cognitive deficits [1]. Due to lacking daily life abilities, Alzheimer's patients always lead to a heavy burden on both families and society. According to the statistical report from Alzheimer's Association, nearly 47 million people worldwide are suffering from AD, and the number of patients will exceed 100 million by 2050 [2]. Therefore, AD is regarded as a severe and urgent public health trouble that needs to be tackled without delay.

For the sake of conquering AD, great efforts have been devoted to develop novel drugs including chemical molecular and biological products by both academic institutions and pharmaceutical companies over the past years [3]. However, most of anti-AD drug candidates with promising therapy effects in the phase of preclinical studies ended up with failure. To date, only four drugs (rivastigmine, galantamine, donepezil, memantine) approved by the US Food and Drug Administration (FDA) are used in clinic. These upset results of developing anti-AD drugs have been attributed to the intricate and multifactorial etiopathogenesis of AD involving deficit of acetylcholine (ACh)[4], β -amyloid protein ($A\beta$) deposits [5], aggregation of Tau protein [6], oxidative stress [7] and metabolic homeostasis disruption of biometals [8]. Thus, the conventional paradigm of 'one drug, one target' may be not suitable enough to treat this complicated disease. To address this issue, a multitarget-directed-ligand (MTDL) strategy means that one molecule that can simultaneously act on multitargets

related to disease, which has been put forward as a potential approach for the treatment of AD [9-11].

Among the therapy targets against AD, acetylcholinesterase (AChE) has been recognized as an important target based on cholinergic hypothesis [12]. The hypothesis emphasizes the deficit of acetylcholine (ACh) in brain regions of Alzheimer's patients leads to memory and cognitive impairments, and reducing the ACh hydrolysis by inhibiting AChE can alleviate these symptoms [13]. At present, with exception of memantine, all FDA-approved drugs are AChE inhibitors (AChEIs). The crystal structure of AChE shows that it consists of two binding sites: one is catalytic anionic site (CAS) and the other is peripheral anionic site (PAS), which are connected by a 20 Å deep gorge [14, 15]. Generally, inhibitors binding to either one site can inhibit AChE. However, recent studies indicate that, in addition to hydrolyzing ACh, AChE also plays a role in inducing the aggregation of A β through the interaction of PAS with A β peptides [16]. Thus, AChE inhibitors, like donepezil, that can simultaneously act on CAS and PAS appear to be more beneficial for AD treatment [17]. Besides AChE, the other cholinesterase isoform, butyrylcholinesterase (BuChE), is also responsible for the ACh hydrolysis. Although several studies have proved that the inhibition of BuChE is another available choice for the treatment of AD, it is still a matter of controversial whether the inhibition on BuChE is safe and effective enough as a treatment approach for AD, because BuChE prevalently distributes in peripheral tissues, and its inhibition may cause peripheral cholinergic side effect [18]. Therefore, the selective inhibition of AChE is more promising for AD

treatment.

In addition to AChE, monoamine oxidase (MAO) is also an efficient therapy target in the treatment of AD. MAO is a flavin adenine dinucleotide (FAD)-containing enzyme that is responsible for the oxidative deamination of various biogenic and xenobiotic amines [19]. Based on substrate selectivity and inhibitor sensitivity, MAO has been classified as two isoforms, namely MAO-A and MAO-B. Typically, MAO-A is selectively and irreversibly inhibited by clorgyline and catalyzes the oxidation of 5-HT, whereas MAO-B is irreversibly inhibited by L-deprenyl and deaminates the benzylamine and 2-phenylethylamine [20]. Accumulated evidence shows that MAO-B activity increases with age, especially in AD patients, a significant activity rise is found in brain tissue, cerebral spinal fluid (CSF) as well as in platelets [21]. The elevated activity of MAO-B leads to an increased level of hydrogen peroxide and oxidative free radicals, which give rise to neuronal damage [22]. Furthermore, the activated MAO-B can also cause disorder of the cholinergic system, destroy cholinergic neurons, and promote the formation of amyloid plaques [23]. Thus, inhibition of MAO-B provides another potential approach for treating AD.

In view of the importance of AChE and MAO-B in the treatment of AD, designing MTDLs with simultaneous inhibition of AChE and MAO-B receive much attention in recent years. A lot of AChE/MAO-B inhibitors with good therapy effect have been reported [24-26]. Among them, ladostigil designed by hybridization of rivastigmine and rasagiline has been announced to enter phase III clinical trials[27], which encourage us to further search for other new multitarget molecules with AChE and

MAO-B inhibitory activity.

Coumarins constitute a large family of natural products, which are widely present in many plant species. In recent years, considerable attention has been paid to coumarins due to their widely biological activities related to neurological disorders, especially for AD [28; 29]. It has been demonstrated that coumarin can inhibit AChE through binding to PAS of AChE [30]. Besides, it can occupy the substrate cavity of MAO-B, and thus presenting potent MAO-B inhibitory activity [31]. Given such excellent properties of coumarin on AChE and MAO-B inhibition, more and more MTDLs with AChE and MAO-B inhibitory activity have been designed and synthesized based on coumarin core [32]. In most cases for design of these MTDLs, the coumarin was chosen to connect with a CAS binding moiety through a flexible linker lodged into the mid-gorge of AChE [33]. Owing to the inhibitory activity of coumarin, the designed compounds can not only exert AChE and MAO-B inhibitory activity but also simultaneously interact with PAS and CAS of AChE. Over the past three years, our group has reported a number of coumarin derivatives as multitarget AChE/MAO-B inhibitors according to this method, and most of them showed promising inhibitory activity [34, 35]. As an ongoing program to development of these multitarget inhibitors, in this work we wanted to introduce new CAS binding moiety to connect with coumarin fragment.

Dithiocarbamate is a versatile pharmacophore with a wide range of biological activity profiles, such as anticancer, antibacterial and inhibition on carbonic anhydrase. Recent years, although dithiocarbamate derivatives have been widely reported, few reports

focus on its activities related to neurodegenerative disease. Very recently, our group found that dithiocarbamate moiety could interact with CAS of AChE [36]. Therefore, we attempted to combine this moiety with coumarin to design a new series of coumarin-dithiocarbamate hybrids as multitarget AChE/MAO-B inhibitors for the treatment of AD. All designed compounds were synthesized and tested *in vitro* to evaluate their inhibitory activities on ChEs and MAOs. The compound with good and balanced inhibitory activity on both AChE and MAO-B was selected for further evaluation including the ability to cross the blood-brain barrier (BBB), *in vitro* toxicity on SH-SY5Y neuroblastoma cell, acute toxicity, and neuroprotective effects in scopolamine-induced cognitive impairment in mice. In addition, kinetic and molecular modeling studies were also conducted to investigate binding mechanism of the selected compound with both AChE and MAO-B.

2. Design of coumarin-dithiocarbamate hybrids

As shown in **Figure 1**, like our previous design, the coumarin moiety was chosen to inhibit the MAO-B and interact with PAS of AChE due to its aromatic character. The dithiocarbamate moiety was used for binding to CAS of AChE. Meanwhile, a flexible linker was utilized to connect these two fragments, which could allow the designed compounds to simultaneously act on CAS and PAS of AChE. In addition, a 3,4-dimethylcoumarin and a piperidine dithiocarbamate moiety were exploited as starting fragments in our initial step, because the previous studies suggested that these two moieties could potently and selectively inhibit MAO-B and AChE, respectively [26, 36]. In order to get optimal linker length for balanced inhibition of AChE and

MAO-B, compounds with varied linker length were synthesized firstly. And once the optimal length was determined, various substitutes and secondary amine groups were, respectively, introduced to coumarin and dithiocarbamate moiety for SAR studies.

3. Results and discussion.

3.1 Chemistry

The synthetic rout for target compounds **7a-n** and **8a-n** is depicted in **Scheme 1-2**. Following the procedures listed in **Scheme 1**, the coumarin derivatives **5a-e** and **5h** were obtained by our previously reported methods [35]. Then, treating 2,4-dihydroxybenzaldehyde with ethyl acetoacetate or diethyl malonate in the presence of piperidine afforded compounds **5f** and **5g**. Before preparation of the cycloalkyl-substituted 7-hydroxycoumarins **5i-k**, the key intermediates **4a-c** were firstly prepared through reacting the corresponding cycloalkanone **3a-c** with diethyl carbonate in the presence of sodium hydride according to the reported procedures[37, 38]. Afterwards, **5i-k** were obtained by the consideration of **4a-c** with resorcinol by using concentrated sulfuric acid as catalyst at 0 °C to room temperature. All synthesized coumarin derivatives **5a-k** were subsequently reacted with the corresponding α , ω -dibromoalkanes to give compounds **6a-n**. Finally, compounds **6a-n** were treated with the appropriate secondary amines, carbon disulfide and triethylamine in DMF to obtain the target compounds **7a-n** and **8a-n** [39].

3.2 *In vitro* biological activity evaluation

The ChEs inhibitory potencies of target compounds **7a-n** and **8a-n** were firstly tested on electric eel acetylcholinesterase (eeAChE) and equine serum butyrylcholinesterase

(eqBuchE) by the Ellman's spectrophotometric method (Table 1-2) [40], then six compounds **7c**, **7g**, **8f-g** and **8j-k** were selected to determine their inhibitory activities towards human acetylcholinesterase (hAChE) owing to their good and selective inhibition on both eeAChE and MAO-B (Table 3). The inhibitory capabilities against MAOs of the tested compounds were assessed directly on human MAOs following a fluorescence-based Amplex Red method [41, 42]. Donepezil and two MAO inhibitors, rasagiline and iproniazid, were used as positive control to reflect the inhibitory potencies of all resulting compounds.

As shown in Table 1 and Table 2, most compounds exhibited potent inhibitory activity on AChE with IC_{50} values ranging from micromolar to nanomolar. Among these compounds, compound **8f** showed the most potent inhibition on eeAChE with IC_{50} value of 0.0068 μ M, which was 6-fold more potent than that of the reference compound donepezil ($IC_{50} = 0.041 \mu$ M). For MAO-B, compounds also presented moderate to good inhibitory activities. Compound **8g** was the most potent inhibitor for MAO-B in this series, showing the IC_{50} value of 0.101 μ M, which was higher than those of rasagiline ($IC_{50} = 0.138 \mu$ M) and iproniazid ($IC_{50} = 7.48 \mu$ M). In addition, all compounds displayed excellent selectivity towards AChE and MAO-B over BuChE and MAO-A. Considering inhibition of BuChE and MAO-A may lead to unexpected side effects in the peripheral tissues, these compounds may be more beneficial for AD treatment. Meanwhile, due to the poor inhibition of compounds on both BuChE and MAO-A, it was difficult to draw a clear structure-activity relationships (SARs) for them. Thus, the discussion of the SARs was mainly made on AChE and MAO-B.

Our previous studies indicated that the linker length tethering coumarin to CAS binding moiety played a crucial role in determining AChE and MAO-B inhibitory activity [34,35]. Therefore, the effect of linker length was firstly investigated by preparing compounds **7a-d** with different linker lengths ($m = 2-5$). It can be seen from the **Table 1** that a pronounced enhancement of inhibitory activity for AChE is observed with progressive elongation of the methylene linker from two to four carbon atoms. Compound **7b** ($IC_{50} = 1.39 \mu\text{M}$) with a three-carbon atom linker provided much better inhibitory activity for AChE than compound **7a** with a two-carbon atom linker ($IC_{50} = 20.85 \mu\text{M}$). When the linker length was extended to four carbon atoms, the obtained compound **7c** ($IC_{50} = 0.082 \mu\text{M}$) presented the most potent inhibitory activity in this subset. However, further lengthening the linker length to five carbon atoms did not lead to an increase in AChE inhibition. Compound **7d** ($IC_{50} = 0.088 \mu\text{M}$) showed a little decreased inhibition compared to compound **7c**. Similar tendency was also found in MAO-B inhibition, in general, compounds with the longer linker displayed stronger inhibitory activity. However, different from AChE inhibition, the linker length with odd number of carbon atoms seemed more beneficial for MAO-B inhibition, as compounds **7d** ($m = 5$) and **7b** ($m = 3$) showed more potent inhibitory activity than compound **7c** ($m = 4$). Notably, compound **7d** with a five-carbon atom linker also exhibited a strong inhibitory activity for MAO-A ($IC_{50} = 0.654 \mu\text{M}$), which indicated that a more flexible linker that was longer than four carbon atoms might give rise to a lower selectivity for MAO-B. In fact, the inhibitory activity on MAO-A can give rise to an unexpected side effect of “cheese reaction” [43]. Therefore, taking

the inhibitory activity and selectivity on both AChE and MAO-B into consideration, the linker containing four carbon atoms ($m = 4$) was chosen as optimal length to connect coumarin and dithiocarbamate moiety.

When the optimal linker length was determined, different substituents were introduced to the position(s) 3 and/or 4 of coumarin ring to explore the possible effects on both enzyme inhibition. As shown in **Table 1**, with exception of compound **7g**, which have a chloro group at position 3 and a methyl group at position 4 of coumarin ring, exhibited improved inhibitory activity on both AChE and MAO-B ($IC_{50} = 0.061 \mu\text{M}$ for AChE; $IC_{50} = 0.363 \mu\text{M}$ for MAO-B), all compounds showed decreased inhibitory activity compared to compound **7c**. The introduction of various substituents to coumarin ring did not have a significant influence on AChE inhibition, as the IC_{50} values of most compounds were varied very closely. Only compound **7k** ($IC_{50} = 15.48 \mu\text{M}$) with a phenyl substituent at 4-position of coumarin led to a large decrease in inhibiting AChE. This suggested that the high steric hindrance on coumarin region could not be well accommodated in active site of AChE. In contrast, a wider activity range could be observed for MAO-B, which indicated that more pronounced effect of the substituents on the MAO-B inhibition. In fact, this result might be consistent with our design that coumarin was the main fragment responsible for MAO-B inhibition.

In comparison to compound **7c**, removing the two methyl groups (**7e**) or 4-substituted methyl group alone (**7f**) on coumarin ring resulted in a decreased activity for MAO-B, which suggested that the methyl group at position 4 of coumarin seemed beneficial

for maintaining the inhibitory activity. Keeping the methyl group at position 4 unchanged and replacing the other methyl group with an electron-withdrawing substituent, chloro group, increased the inhibition for MAO-B. The obtained compound **7g** was found to be the strongest inhibitor in this series. However, introduction of a strong electron-withdrawing substituent, trifluoromethyl group, to coumarin ring afforded compound **7h**, which gave the poorest activity in this series ($IC_{50} = 42.12 \mu M$). Unlike previous reports that introducing methyl ketone or ethyl ester group to position 3 of coumarin moiety could improve the inhibitory activity on MAO-B[44], compounds **7i** ($IC_{50} = 12.29 \mu M$) and **7j** ($IC_{50} = 39.0 \mu M$) displayed weak inhibition in our present study. Moreover, like AChE inhibition, the presence of a phenyl group at 4-position of coumarin was also not favorable for MAO-B inhibition. Compound **7k** ($IC_{50} = 17.57 \mu M$), which possess a bulky phenyl group on coumarin ring, exerted a less inhibitory activity for MAO-B. In addition, given the above results that compounds bearing di-substitution pattern on 3 and 4- positions of coumarin showed more potent inhibition for MAO-B in comparison to mono-substituted compounds, three compounds **7l-n** with different size of 3, 4-fused cyclic substituents were also synthesized to further extend the SARs. Among these compounds, compound **7m** ($IC_{50} = 1.24 \mu M$) having a six-membered ring on coumarin was more potent than its homologues **7l** ($IC_{50} = 4.0 \mu M$) and **7n** ($IC_{50} = 21.40 \mu M$), which suggested that the spatial arrangement of cyclohexyl allows for a better positioning in the active site of the MAO-B. After completing these investigations, compound **7g** with good and balanced inhibitory activity on AChE and MAO-B was fished out for

further modification.

Compounds **8a-n** were designed to explore the influences of different terminal amine groups on inhibitory activity towards the target enzymes. Initially, we thought that changing the dithiocarbamate moiety of compound **7g** would mainly impact the AChE inhibition, because this moiety was designed as a CAS binding moiety to interact with AChE. However, to our surprise, the replacement of terminal piperidyl group in compound **7g** with other secondary amine groups also led to great impact on the inhibition for MAO-B. Substituted piperidine groups were firstly introduced to investigate their effects on inhibitory activity. Compounds **8a-e** were obtained by modification at position 4 of piperidine with different substituents. Compared to unsubstituted piperidine compound **7g**, introduction of corresponding 4-substituents resulted in a dramatic reduced inhibitory activity against AChE, which made the IC_{50} values range from 1.54 μ M (**8c**) to 18.46 μ M (**8b**). The similar negative effect on inhibitory activity towards MAO-B was also observed, as four out of five compounds (**8a-e**) displayed much lower activities than compound **7g**. Among them, compound **8b** bearing 4-phenylpiperidine presented the worst inhibitory activity on both AChE and MAO-B ($IC_{50} = 18.46 \mu$ M for AChE; $IC_{50} = 31.12 \mu$ M for MAO-B). However, introduction of 4-methyl group to piperidine (**8e**) brought a significant potency improvement on MAO-B ($IC_{50} = 0.347 \mu$ M), which proved that methyl group might be a potential substituent to keep the good inhibitory activity on MAO-B. Shifting the methyl group from position 4 to position 2 of piperidine led to compound **8f** ($IC_{50} = 0.0068 \mu$ M), giving a highly surprise that this minor change resulted in a 650-fold

improvement in AChE inhibition. Conversely, the MAO-B inhibitory activity of compound **8f** was 2.5-fold decreased compared to 4-methylpiperidyl hybrid **8e** (**8f**: $IC_{50} = 0.876 \mu\text{M}$ vs **8e**: $IC_{50} = 0.347 \mu\text{M}$), which indicated the ortho-methyl substitution of the nitrogen atom in piperidine played a pivotal role in the inhibitory activity for AChE and MAO-B. Further installation of another methyl group to position 6 of piperidine ring obtained 2, 6-dimethylpiperidinyl derivative **8g**. Although this compound exhibited less AChE inhibitory activity than **8f**, its activity on MAO-B was remarkably improved. Such change rendered compound **8g** ($IC_{50} = 0.044 \mu\text{M}$ for AChE; $IC_{50} = 0.101 \mu\text{M}$ for MAO-B) a more balanced inhibitor than compound **7g**.

The effects of replacement of the piperidine group with other alkyl amines or cyclic amines were also explored by preparing compounds **8h-n**. The alkyl amine compounds **8h-j** showed continuous enhancement to both AChE and MAO-B inhibition with gradually increasing the alkyl groups. Compound **8j** ($IC_{50} = 0.167 \mu\text{M}$ for AChE; $IC_{50} = 0.788 \mu\text{M}$ for MAO-B) bearing a diethylamine group exhibited more potent activity than its congeners **8h** ($IC_{50} = 11.67 \mu\text{M}$ for AChE; $IC_{50} = 2.07 \mu\text{M}$ for MAO-B) and **8i** ($IC_{50} = 0.217 \mu\text{M}$ for AChE; $IC_{50} = 7.49 \mu\text{M}$ for MAO-B).

Contraction of the piperidine ring to pyrrole ring produced compound **8k** ($IC_{50} = 0.386 \mu\text{M}$ for AChE; $IC_{50} = 0.542 \mu\text{M}$ for MAO-B), which resulted in a little decrease in both AChE and MAO-B inhibition compared to compound **7g**. However, inserting oxygen or nitrogen atoms into piperidine ring, affording compounds **8l-n**, led to a dramatic drop in both enzyme inhibitory activity. Especially for MAO-B, the IC_{50}

values of compounds **8l-n** were found to be higher than 25 μM . This suggested that the presence of heteroatoms at terminal of piperidine ring was not tolerated for compound locating into active sites of both AChE and MAO-B.

3.3 *In vitro* inhibition on human ChEs

In order to evaluate the inhibitory activities of designed compounds on ChEs more reasonably, six compounds **7c**, **7g**, **8f-g**, and **8j-k** having relatively good inhibitory activity and selectivity on eeAChE and MAO-B were selected for further assay on human AChE. From the **Table 3**, it can be seen that all of them still maintain the high inhibitory activity and excellent selectivity on hAChE with IC_{50} values ranging from sub-micromolar to low nanomolar. In particular, compound **8f** with best inhibition on eeAChE also presented the most potent inhibitory activity on hAChE. It showed the IC_{50} value of 0.0089 μM , which was nearly 2.4-fold more potent than that of donepezil ($\text{IC}_{50} = 0.021 \mu\text{M}$) under the same conditions.

3.4 *In vitro* blood-brain barrier permeation assay

The good permeability for blood-brain barrier (BBB) is a significant factor for drugs that can successfully act on the central nervous system (CNS). Thus, it is essential to investigate whether the present compounds could penetrate the BBB. Compounds **7c**, **7g**, **8f-g** and **8j-k** with strong inhibitory activity on both hAChE and hMAO-B were selected to determine their permeabilities for BBB by the parallel artificial membrane permeation assay of blood-brain barrier (PAMPA-BBB)[45]. The permeability of 9 commercial drugs with their reported values were used to validate the assay (**Table 4**). A plot of experimental data *versus* the reported values gave a good linear correlation,

P_e (exp.) = 0.9050 P_e (bibl.) - 0.2568 ($R^2 = 0.9759$) (**Figure 2**). From this equation and considering the limit established by Di et al. for BBB permeation, we determined the following ranges of permeability: compound with P_e ($\times 10^6$ cm/s) > 3.36 represented high BBB permeation (CNS+), compound with P_e ($\times 10^6$ cm/s) < 1.55 represented low BBB permeation (CNS-), compound with $1.55 < P_e$ ($\times 10^6$ cm/s) < 3.36 represented uncertain BBB permeation (CNS \pm). It can be seen from the **Table 5** that, with exception of compound **8f** that shows an uncertain BBB permeation, all compounds exhibit P_e ($\times 10^6$ cm/s) values higher than 3.36, suggesting that they can cross the BBB and may reach the therapeutic target in CNS. After all above biological evaluation, compound **8g** possessing good BBB permeability as well as potent and well-balanced inhibition on hAChE and hMAO-B ($IC_{50} = 0.114$ and 0.101 μ M, respectively) was selected as the optimal candidate for further study.

3.5 Kinetic study of inhibition on AChE.

In order to investigate the inhibition mechanism of compound **8g**, an enzyme kinetic study was carried out on hAChE. After plotting the reciprocal of enzyme velocity ($1/v$) versus the reciprocal of substrate concentration ($1/S$), the established Lineweaver-Burk reciprocal plots showed that both increasing slopes and intercepts at increasing inhibitor concentration (37, 74 and 148 nM) (**Figure 3**). The pattern suggested that there was a mixed-type inhibition mechanism between hAChE and compound **8g**, which implied that **8g** might be able to interact with both catalytic active site (CAS) and peripheral anionic site (PAS) of AChE.

3.6 Reversibility and kinetic study of hMAO-B inhibition

As we know, reversible inhibitors of MAO-B have superior advantages over the irreversible inhibitors in the view of AD treatment. Thus, investigating whether compound **8g** is a/an reversible or irreversible inhibitor of MAO-B is very necessary. The investigation was carried out by recovering the enzymatic activity after dilution of the enzyme-inhibitor complexes, and an irreversible inhibitor, pargyline, was used as reference compound[46]. Before starting experiment, MAO-B was pre-incubated with compound **8g** at concentrations of 0, 10 and $100 \times IC_{50}$ for 30 min. Then, these incubations were diluted 100-fold to obtain concentrations of 0, 0.1 and $1 \times IC_{50}$. If compound is a reversible inhibitor, enzymatic activity is expected to recover to approximately 90 % after dilution to $0.1 \times IC_{50}$, and 50 % after dilution to $1 \times IC_{50}$. If compound is an irreversible inhibitor, enzymatic activity is expected not to recover after diluting the enzyme-inhibitor complex. As shown in **Figure 4**, after diluting compound **8g** to $0.1 \times IC_{50}$ and $1 \times IC_{50}$, the MAO-B catalytic activities are recovered to levels of 87 % and 46% of control value, respectively. This behavior suggested that compound **8g** was a reversible inhibitor for MAO-B. In contrast, after incubation of MAO-B with the irreversible inhibitor pargyline at $10 \times IC_{50}$, and dilution of it to $0.1 \times IC_{50}$, the enzyme activity was not recovered (less than 10% of control).

To further explore the interaction mechanism of compound **8g** with hMAO-B, an enzyme kinetic study similar as AChE was carried out. The Lineweaver-Burk reciprocal plots were established according to initial rates of the MAO-B-catalyzed oxidation for different concentrations of *p*-tyramine in the presence of three different concentrations (63, 126, and 252 nM) of compound **8g** (**Figure 5**). The plots were

linear and intersected at the y-axis, which indicated compound **8g** was a competitive inhibitor for hMAO-B.

3.7. Molecular modeling studies

To further study the binding modes of compound **8g** with hAChE and hMAO-B, docking studies were performed using the Molecular Operating Environment (MOE 2008.10) software package.

3.7.1 Docking study of compounds **8g** with hAChE

The docking mode of **8g** on hAChE was investigated based on the X-ray crystal structure of the recombinant human acetylcholinesterase (hAChE) complexed with donepezil (PDB code 4EY7). As shown in **Figure 6**, similar to our previous study, the coumarin moiety can occupy the PAS of hAChE and establish a π - π stacking interaction between its phenyl ring and the indole ring of Trp 286 (3.75 Å). In the middle gorge, the side chain connecting coumarin with dithiocarbamate moiety folded in a conformation in gorge that allowed it to interact with Phe 338, Tyr 341 and Phe 297 *via* hydrophobic interactions. Besides, the oxygen atom in the side chain also formed a hydrogen bond with the residue Tyr 124 in middle gorge (3.20 Å), which further enhanced the binding ability to mid-gorge site. At last, the piperidinyldithiocarbamate moiety of compound **8g** was bound to the CAS, exhibiting a hydrophobic interaction with residues Gly 448, Trp 86, Tyr 337, His 447 and Gly 121. Taken together, all these results suggested that compound **8g** could occupy the entire enzyme active sites and is a dual binding site inhibitor to hAChE.

3.7.2 Docking study of compounds **8g** with hMAO-B

The binding mode of compound **8g** with respect to MAO-B was investigated based on the X-ray crystal structure of the human monoamine oxidase B (hMAO-B) in complex with 7-(3-chlorobenzyloxy)-4-(methylamino)methyl-coumarin (PDB code 2V61). It can be seen from the **Figure 7** that compound **8g** crosses both the substrate cavity and the entrance cavity of MAO-B. The coumarin moiety was located into the substrate cavity, which left the lactone ring close to the FAD cofactor, and it was stabilized by hydrophobic interactions with Tyr 398, Phe 343, Tyr 60 and Tyr 435. Besides, the carbonyl oxygen of coumarin moiety also formed a hydrogen bond with Tyr 188 (2.84 Å). The piperidinyldithiocarbamate moiety occupied the entrance cavity and interacted with Phe 168, Leu 167, Leu 164, Pro 102, Pro 104, Ile 316, Trp199 and Phe 103 through van der waals and hydrophobic interactions.

Overall, the above docking studies of compound **8g** with both hAChE and hMAO-B provided an explanation for kinetic assays and demonstrated the rationality of our molecular design.

3.8 Cytotoxicity of human neuroblastoma SH-SY5Y cells.

In order to evaluate the safety of compound **8g**, cell toxicity experiment was performed on human neuroblastoma cells SH-SY5Y, and donepezil was taken as the reference compound. After treatment of SH-SY5Y cells with different concentrations of compound **8g** or donepezil for 24 h, the cell viability was determined by 3-(4,5-dimethylthiazol-2-yl)-2, 5-diphenyltetrazolium (MTT) assay[47]. As shown in **Figure 8**, compound **8g**, like donepezil, shows negligible toxicity to SH-SY5Y cells at test concentrations (6.25-100 µM), which indicate that it is a safe agent for the

treatment of AD.

3.9. Acute toxicity study

Acute toxicity of compound **8g** was carried out on KM mice (n = 10 per group, half male and half female) according to the reported method[48]. Compound **8g** was delivered to mice by oral administration at three doses of 625, 1250 and 2500 mg/kg. After drug administration, mice were observed continuously for the first 4 h for any abnormal behavior and mortality changes, intermittently for the next 24 h, and occasionally thereafter for 14 days for the onset of any delayed effects. During the treatment period, no toxicity effects such as death, body weight reduction (**Figure 9**), obvious decline in water or food consumption, or significant abnormal behaviors were observed. In addition, all animals were sacrificed on the 14th day, and possible toxic damage on heart, liver and kidneys was examined macroscopically. The results indicated that compound **8g** did not cause any toxic effect on mice at dose up to 2500 mg/kg.

3.10. In vivo efficacy evaluation

The satisfactory therapeutic results in vitro of compound **8g** encouraged us to further determine whether it could improve memory impairment in vivo. The therapeutic effect of compound **8g** was tested using the scopolamine-induced cognitive deficit mouse model [49]. A step-down passive avoidance test was performed to provide an evaluation on the effect of cognitive improvement by compound **8g** [50], and the marketed drug, donepezil, was used as positive reference. As shown in **Figure 10**, the model group present much shorter latency and more number of errors than control

group ($### P < 0.001$). With exception of the low dose group of compounds **8g**, the latency and number of errors of all groups exhibited a significant difference compared to model group ($** P < 0.01$, $*** P < 0.001$, respectively). After treatment with compound **8g**, the latency and number of errors were reversed in a dose-dependent manner. High dose group (20 mg/kg) and medium dose group (10 mg/kg) exhibited longer latencies (134.9 s, 127.1 s vs 122.7s) and less number of errors (1.25, 1.4, vs 1.6) than donepezil group (10 mg/kg). Although the low dose group (5mg/kg) did not present significant difference with the model group, the latency and number of errors were obviously improved (94.8 s vs 63.2s, 2.75 vs 3.83). This in vivo study further proved that compound **8g** might be a promising compound for the treatment of AD.

4. Conclusion

In this study, a series of new hybrids based on coumarin and dithiocarbamate scaffolds were designed, synthesized and evaluated as multitarget AChE/MAO-B inhibitors. The results indicated that most of designed compounds exhibited potent and selective inhibitory activity on AChE and MAO-B. The SAR analysis suggested that the linker length between coumarin and dithiocarbamate moieties played an important role in both AChE and MAO-B inhibition, and the four-carbon atom linker was the optimal length for compound that potently and selectively inhibited the both enzymes. The substituents on coumarin moiety showed more significantly effects on MAO-B inhibition than those on AChE, and the di-substitution pattern on coumarin seemed more beneficial for improving the inhibitory activity of MAO-B. In contrast, the terminal amine groups could largely influence the inhibitory activity for both AChE

and MAO-B. Compounds with piperidine or methyl-substituted piperidines were more favorable to the inhibitory activity. Interestingly, the position of methyl substitution on piperidine group has an essential effect on inhibiting AChE. When the methyl group was shifted from 4-position to 2-position of the piperidine ring, a 650-fold improvement in AChE inhibition was observed, and the obtained compound **8f** presented the most potent AChE inhibitory activity in this series ($IC_{50} = 0.0068 \mu M$ for eeAChE; $IC_{50} = 0.0089 \mu M$ for hAChE).

Of these compounds, compound **8g** with potent and balanced inhibitory activity for AChE and MAO-B as well as good ability to penetrate the BBB was selected as a promising compound for further studies. Kinetic and molecular modeling study suggested compound **8g** was a mixed-type inhibitor, binding simultaneously to CAS, PAS and mid-gorge site of AChE, and it was also a competitive inhibitor, which could occupy the substrate and entrance cavities of MAO-B. In vitro cytotoxicity assay indicated that compound **8g** showed no toxicity to SH-SY5Y cells at 6.25–100 μM . More importantly, our in vivo study proved that **8g** did not display any acute toxicity in mice at doses up to 2500 mg/kg, and mice treated with **8g** (20 and 10 mg/kg, p.o.) could significantly prolong the latency and reduce number of errors in the step-down passive avoidance test. Taken together, these results highlighted compound **8g** as a potential multitarget agent for the treatment of AD. As far as we know, dithiocarbamate moiety have never been used for design of multitarget AChE/MAO-B inhibitors. Therefore, these results may provide a starting point for design of new multitarget AChE/MAO-B inhibitors based on dithiocarbamate scaffold.

5. Experimental section

5.1 Chemistry

Starting chemical reagents and solvents used in synthesis were purchased from Sinopharm Chemical Reagent Co., Ltd. (China). The reaction progress was routinely checked by thin layer chromatography (TLC) on glass-packed precoated silica gel GF254 (Qingdao Haiyang Chemical Plant, Qingdao, China) plates. Column chromatography was performed using silica gel (90-150 μm ; Qingdao Marine Chemical Inc.). IR spectra were obtained with a PerkinElmer Spectrum Two spectrophotometer (KBr disks). ^1H NMR spectra (600 MHz) and ^{13}C NMR spectra (151MHz) were recorded on a Bruker ACF-600 spectrometer at room temperature using CDCl_3 or $\text{DMSO}-d_6$ as the solvent. Chemical shifts (δ) are reported in parts per million (ppm) using the tetramethylsilane (TMS) as internal standard. The coupling constants J are presented in hertz (Hz). Proton coupling patterns were expressed with following abbreviations: s (singlet), d (doublet), dd (doublet of doublet), t (triplet), m (multiplet), br s (broad signal). Melting points were measured on an XT-4 micromelting point apparatus and are uncorrected. The purity of all compounds for biological evaluation was confirmed to be higher than 95% by analytical HPLC performed on a Waters ACQUITY Arc HPLC system equipped with a 2998 PDA detector. (Column: Hypersil ODS2, 5 μm particle size, 4.6 mm \times 150 mm; mobile phase: A = CH_3OH , B = H_2O , isocratic elution, A = 70%; flow rate = 1 mL/min; λ = 254 nm; 10 μL injection). High resolution mass spectra were conducted on an AB Sciex Triple TOF 5600 spectrometer (HR-ESI-MS).

Synthetic procedures and spectroscopic data of all the intermediates **4a-c**, **5a-k** and **6a-n** are available as Supporting Information.

5.2. General procedure for synthesis of final compounds **7a-n**.

To a mixture of piperidine (1.69 mmol) and triethylamine (1.54 mmol) dissolved in N, N-dimethylformamide (DMF), carbon disulfide (1.85 mmol) was added dropwise. The mixture was stirred for 5 min and a solution of **6a-n** (1.54 mmol) in N, N-dimethylformamide was added. The reaction was allowed to stir for 12 h at room temperature. When the reaction was completed, 30 mL of water was added and the mixture was extracted with ethyl acetate (4 × 18 mL). The ethyl acetate layer was collected, dried over anhydrous sodium sulfate, filtered and then evaporated to dryness to give crude product, which was purified by silica gel column chromatography using petroleum ether/ ethyl acetate (8 : 1 to 15:1) as eluent.

5.2.1. 2-((3,4-dimethyl-2-oxo-2H-chromen-7-yl)oxy)ethyl piperidine-1-carbodi-thioate (**7a**)

Yield 84%; white solid; m.p. 139-140 °C; IR (KBr): $\nu = 2944, 2853, 1714, 1612, 1508, 1478, 1450, 1432, 1283, 1231, 1182, 1091, 857, 755 \text{ cm}^{-1}$. $^1\text{H NMR}$ (600 MHz, CDCl_3) δ : 7.49 (d, $J = 8.9 \text{ Hz}$, 1H), 6.90 (dd, $J = 8.9, 2.5 \text{ Hz}$, 1H), 6.84 (d, $J = 2.5 \text{ Hz}$, 1H), 4.30 (t, $J = 6.4 \text{ Hz}$, 4H), 3.91 (br s, 2H), 3.78 (t, $J = 6.4 \text{ Hz}$, 2H), 2.37 (s, 3H), 2.18 (s, 3H), 1.77 – 1.61 (m, 6H). $^{13}\text{C NMR}$ (151 MHz, CDCl_3) δ : 194.43, 162.41, 160.46, 153.48, 146.16, 125.29, 119.11, 114.46, 112.12, 101.77, 67.02, 53.30, 51.49, 35.57, 29.71, 25.44, 24.26, 15.09, 13.19. HRMS: calcd for $\text{C}_{19}\text{H}_{24}\text{NO}_3\text{S}_2$ $[\text{M} + \text{H}]^+$ 378.1119, found 378.1150. HPLC purity, 99.44%.

5.2.2. *3-((3,4-dimethyl-2-oxo-2H-chromen-7-yl)oxy)propyl piperidine-1-carbodithioate (7b)*

Yield 87%; white solid; m.p. 138-139 °C; IR (KBr): $\nu = 2940, 2859, 1695, 1607, 1510, 1475, 1427, 1286, 1241, 1177, 1086, 859, 761 \text{ cm}^{-1}$. ^1H NMR (600 MHz, DMSO) δ : 7.70 (d, $J = 9.6 \text{ Hz}$, 1H), 6.96 (dd, $J = 9.6, 2.5 \text{ Hz}$, 1H), 6.94 (d, $J = 2.5 \text{ Hz}$, 1H), 4.22 (br s, 2H), 4.15 (t, $J = 6.2 \text{ Hz}$, 2H), 3.90 (br s, 2H), 3.39 (t, $J = 7.2 \text{ Hz}$, 2H), 2.37 (s, 3H), 2.15 – 2.09 (m, 2H), 2.08 (s, 3H), 1.69 – 1.61 (m, 2H), 1.60 – 1.54 (m, 4H). ^{13}C NMR (151 MHz, DMSO) δ : 193.93, 161.72, 160.93, 153.49, 147.32, 126.65, 118.36, 114.14, 112.82, 101.42, 67.32, 52.76, 51.36, 33.25, 28.46, 24.03, 24.03, 22.87, 15.39, 13.38. HRMS: calcd for $\text{C}_{20}\text{H}_{26}\text{NO}_3\text{S}_2$ $[\text{M} + \text{H}]^+$ 392.1276, found 392.1312. HPLC purity, 98.65%.

5.2.3. *4-((3,4-dimethyl-2-oxo-2H-chromen-7-yl)oxy)butyl piperidine-1-carbodithioate (7c)*

Yield 89%; white solid; m.p. 89-91 °C; IR (KBr): $\nu = 2937, 2853, 1702, 1617, 1564, 1502, 1426, 1296, 1241, 1156, 1090, 845, 759 \text{ cm}^{-1}$. ^1H NMR (600 MHz, CDCl_3) δ : 7.47 (d, $J = 8.8 \text{ Hz}$, 1H), 6.83 (dd, $J = 8.8, 2.5 \text{ Hz}$, 1H), 6.78 (d, $J = 2.5 \text{ Hz}$, 1H), 4.30 (t, $J = 6.7 \text{ Hz}$, 2H), 4.04 (t, $J = 5.9 \text{ Hz}$, 2H), 3.89 (br s, 2H), 3.39 (t, $J = 7.1 \text{ Hz}$, 2H), 2.36 (s, 3H), 2.17 (s, 3H), 2.02 – 1.84 (m, 4H), 1.76 – 1.60 (m, 6H). ^{13}C NMR (151 MHz, CDCl_3) δ : 195.59, 162.53, 160.94, 153.56, 146.30, 125.22, 118.86, 114.14, 112.44, 101.14, 67.89, 52.93, 51.30, 36.67, 29.71, 28.28, 25.99, 25.56, 24.33, 15.09, 13.16. HRMS: calcd for $\text{C}_{21}\text{H}_{28}\text{NO}_3\text{S}_2$ $[\text{M} + \text{H}]^+$ 406.1432, found 406.1472. HPLC purity, 99.71%.

5.2.4. *5-((3,4-dimethyl-2-oxo-2H-chromen-7-yl)oxy)pentyl piperidine-1-carbodithioate (7d)*

Yield 86%; white solid; m.p. 91-92 °C; IR (KBr): $\nu = 2938, 2853, 1719, 1606, 1504, 1470, 1431, 1290, 1241, 1182, 1093, 859, 761 \text{ cm}^{-1}$. ^1H NMR (600 MHz, DMSO) δ : 7.67 (d, $J = 9.5 \text{ Hz}$, 1H), 6.92 (dd, $J = 9.5, 2.6 \text{ Hz}$, 1H), 6.91 (d, $J = 2.6 \text{ Hz}$, 1H), 4.20 (br s, 2H), 4.05 (t, $J = 6.4 \text{ Hz}$, 2H), 3.87 (br s, 2H), 3.25 (t, $J = 7.3 \text{ Hz}$, 2H), 2.35 (s, 3H), 2.06 (s, 3H), 1.80 – 1.71 (m, 2H), 1.71 – 1.59 (m, 4H), 1.60 – 1.46 (m, 6H). ^{13}C NMR (151 MHz, DMSO) δ : 194.39, 161.73, 161.17, 153.51, 147.33, 126.59, 118.23, 113.98, 112.76, 101.34, 68.44, 52.71, 51.27, 36.56, 28.65, 28.51, 25.30, 24.05, 24.05, 22.87, 15.37, 13.36. HRMS: calcd for $\text{C}_{22}\text{H}_{30}\text{NO}_3\text{S}_2$ $[\text{M} + \text{H}]^+$ 420.1589, found 420.1608. HPLC purity, 97.71%.

5.2.5. *4-((2-oxo-2H-chromen-7-yl)oxy)butyl piperidine-1-carbodithioate (7e)*

Yield 87%; white solid; m.p. 83-85 °C; IR (KBr): $\nu = 2937, 2851, 1743, 1602, 1578, 1500, 1480, 1283, 1234, 1148, 1079, 864, 752 \text{ cm}^{-1}$. ^1H NMR (600 MHz, CDCl_3) δ : 7.64 (d, $J = 9.4 \text{ Hz}$, 1H), 7.37 (d, $J = 8.6 \text{ Hz}$, 1H), 6.84 (dd, $J = 8.6, 2.3 \text{ Hz}$, 1H), 6.80 (d, $J = 2.3 \text{ Hz}$, 1H), 6.24 (d, $J = 9.4 \text{ Hz}$, 1H), 4.30 (br s, 2H), 4.07 (t, $J = 6.0 \text{ Hz}$, 2H), 3.90 (br s, $J = 6.0 \text{ Hz}$, 2H), 3.40 (t, $J = 7.1 \text{ Hz}$, 2H), 2.01 – 1.88 (m, 4H), 1.78 – 1.59 (m, 6H). ^{13}C NMR (151 MHz, CDCl_3) δ : 195.50, 162.24, 161.27, 155.88, 143.48, 128.76, 112.98, 112.93, 112.48, 101.41, 68.04, 52.92, 51.30, 36.60, 29.70, 28.21, 26.00, 25.55, 24.32. HRMS: calcd for $\text{C}_{19}\text{H}_{24}\text{NO}_3\text{S}_2$ $[\text{M} + \text{H}]^+$ 378.1119, found 378.1166. HPLC purity, 98.63%.

5.2.6. *4-((3-methyl-2-oxo-2H-chromen-7-yl)oxy)butyl piperidine-1-carbodithioate (7f)*

Yield 80%; white solid; m.p. 105-107 °C; IR (KBr): $\nu = 2934, 2862, 1716, 1620, 1570, 1507, 1476, 1293, 1224, 1148, 1074, 849, 750 \text{ cm}^{-1}$. ^1H NMR (600 MHz, DMSO) δ : 7.79 (s, 1H), 7.51 (d, $J = 8.6 \text{ Hz}$, 1H), 6.94 (d, $J = 2.2 \text{ Hz}$, 1H), 6.90 (dd, $J = 8.6, 2.2 \text{ Hz}$, 1H), 4.21 (t, $J = 6.4 \text{ Hz}$, 2H), 4.07 (t, $J = 6.1 \text{ Hz}$, 2H), 3.87 (br s, 2H), 3.30 (t, $J = 7.0 \text{ Hz}$, 2H), 2.04 (s, 3H), 1.87 – 1.73 (m, 4H), 1.67 – 1.59 (m, 2H), 1.58 – 1.49 (m, 4H). ^{13}C NMR (151 MHz, DMSO) δ : 194.23, 162.06, 161.21, 154.81, 140.30, 128.94, 121.47, 113.27, 113.09, 101.33, 68.19, 52.75, 51.30, 36.30, 30.46, 28.13, 26.23, 25.65, 24.04, 16.94. HRMS: calcd for $\text{C}_{20}\text{H}_{26}\text{NO}_3\text{S}_2$ $[\text{M} + \text{H}]^+$ 392.1276, found 392.1348. HPLC purity, 99.32%.

5.2.7. *4-((3-chloro-4-methyl-2-oxo-2H-chromen-7-yl)oxy)butyl piperidine-1-carbodithioate (7g)*

Yield 89%; yellow solid; m.p. 119-121 °C; IR (KBr): $\nu = 2941, 2854, 1730, 1600, 1508, 1471, 1433, 1288, 1245, 1143, 1076, 830, 753 \text{ cm}^{-1}$. ^1H NMR (600 MHz, CDCl_3) δ : 7.51 (d, $J = 8.9 \text{ Hz}$, 1H), 6.89 (dd, $J = 8.9, 2.5 \text{ Hz}$, 1H), 6.81 (d, $J = 2.5 \text{ Hz}$, 1H), 4.30 (br s, 2H), 4.06 (t, $J = 6.0 \text{ Hz}$, 2H), 3.89 (br s, 2H), 3.39 (t, $J = 7.1 \text{ Hz}$, 2H), 2.54 (s, 3H), 2.02 – 1.84 (m, 4H), 1.78 – 1.61 (m, 6H). ^{13}C NMR (151 MHz, CDCl_3) δ : 195.50, 161.98, 157.50, 153.13, 148.01, 125.85, 117.71, 113.33, 113.23, 101.33, 68.11, 52.91, 51.28, 36.58, 29.71, 28.19, 25.98, 25.56, 24.33, 16.19. HRMS: calcd for $\text{C}_{20}\text{H}_{25}\text{ClNO}_3\text{S}_2$ $[\text{M} + \text{H}]^+$ 426.0886, found 426.0934. HPLC purity, 99.02%.

5.2.8. *4-((2-oxo-4-(trifluoromethyl)-2H-chromen-7-yl)oxy)butyl piperidine-1-carbodithioate (7h)*

Yield 84%; white solid; m.p. 111-113 °C; IR (KBr): $\nu = 2937, 2860, 1736, 1610, 1514,$

1472, 1430, 1346, 1284, 1240, 1123, 1033, 852 cm^{-1} . ^1H NMR (600 MHz, CDCl_3) δ : 7.61 (d, $J = 9.0$ Hz, 1H), 6.92 (dd, $J = 9.0, 2.5$ Hz, 1H), 6.86 (d, $J = 2.5$ Hz, 1H), 6.61 (s, 1H), 4.30 (br s, 2H), 4.09 (t, $J = 6.1$ Hz, 2H), 3.90 (br s, 2H), 3.40 (t, $J = 7.2$ Hz, 2H), 2.05 – 1.86 (m, 4H), 1.79 – 1.61 (m, 6H). ^{13}C NMR (151 MHz, CDCl_3) δ : 195.44, 162.96, 159.48, 156.35, 141.62 (q, $J = 32$ Hz), 126.32, 121.63 (q, $J = 273$ Hz), 113.73, 112.11, 106.97, 101.92, 68.25, 52.96, 51.29, 36.52, 29.71, 28.11, 25.94, 25.55, 24.26. HRMS: calcd for $\text{C}_{20}\text{H}_{23}\text{F}_3\text{NO}_3\text{S}_2$ $[\text{M} + \text{H}]^+$ 446.0993, found 446.1039. HPLC purity, 99.21%.

5.2.9. 4-((3-acetyl-2-oxo-2H-chromen-7-yl)oxy)butyl piperidine-1-carbodithioate (**7i**)

Yield 84%; yellow solid; m.p. 128-130 $^\circ\text{C}$; IR (KBr): $\nu = 2920, 2853, 1725, 1677, 1613, 1503, 1471, 1279, 1214, 1142, 1036, 868, 770$ cm^{-1} . ^1H NMR (600 MHz, CDCl_3) δ : 8.49 (s, 1H), 7.53 (d, $J = 8.7$ Hz, 1H), 6.89 (dd, $J = 8.7, 2.3$ Hz, 1H), 6.81 (d, $J = 2.3$ Hz, 1H), 4.30 (br s, 2H), 4.11 (t, $J = 6.1$ Hz, 2H), 3.90 (br s, 2H), 3.40 (t, $J = 7.2$ Hz, 2H), 2.71 (s, 3H), 2.04 – 1.86 (m, 4H), 1.80 – 1.53 (m, 6H). ^{13}C NMR (151 MHz, CDCl_3) δ : 195.58, 195.44, 164.71, 159.82, 157.79, 147.85, 131.50, 120.55, 114.21, 111.98, 100.80, 68.40, 52.96, 51.33, 36.49, 31.94, 30.61, 29.71, 28.10, 25.56, 24.32. HRMS: calcd for $\text{C}_{21}\text{H}_{25}\text{NO}_4\text{S}_2$ $[\text{M} + \text{Na}]^+$ 442.1025, found 442.1081. HPLC purity, 98.97%.

5.2.10. Ethyl 2-oxo-7-(4-((piperidine-1-carbonothioyl)thio)butoxy)-2H-chromene-3-carboxylate (**7j**)

Yield 87%; white solid; m.p. 113-114 $^\circ\text{C}$; IR (KBr): $\nu = 2927, 2856, 1748, 1692, 1615, 1550, 1500, 1485, 1286, 1223, 1143, 1043, 861, 795$ cm^{-1} . ^1H NMR (600 MHz,

CDCl₃) δ : 8.50 (s, 1H), 7.49 (d, $J = 8.7$ Hz, 1H), 6.88 (dd, $J = 8.7, 2.3$ Hz, 1H), 6.80 (d, $J = 2.3$ Hz, 1H), 4.40 (q, $J = 7.1$ Hz, 2H), 4.30 (br s, 2H), 4.10 (t, $J = 6.1$ Hz, 2H), 3.90 (br s, 2H), 3.40 (t, $J = 7.2$ Hz, 2H), 2.02 – 1.86 (m, 4H), 1.78 – 1.62 (m, 6H), 1.40 (t, $J = 7.2$ Hz, 3H). ¹³C NMR (151 MHz, CDCl₃) δ : 195.43, 164.57, 163.50, 157.57, 157.21, 149.02, 130.70, 113.98, 111.57, 100.88, 68.35, 61.70, 52.96, 51.29, 36.51, 31.93, 29.70, 28.09, 25.97, 25.54, 24.32, 14.30. HRMS: calcd for C₂₂H₂₈NO₅S₂ [M + H]⁺ 450.1331, found 450.1407. HPLC purity, 98.64%.

5.2.11. *4-((2-oxo-4-phenyl-2H-chromen-7-yl)oxy)butyl piperidine-1-carbodithioate (7k)*

Yield 81%; white solid; m.p. 115-116 °C; IR (KBr): $\nu = 3075, 2934, 2849, 1715, 1602, 1471, 1429, 1281, 1231, 1157, 1043, 860, 754$ cm⁻¹. ¹H NMR (600 MHz, CDCl₃) δ : 7.53 – 7.49 (m, 3H), 7.46 – 7.42 (m, 2H), 7.37 (d, $J = 8.9$ Hz, 1H), 6.88 (d, $J = 2.5$ Hz, 1H), 6.79 (dd, $J = 8.9, 2.5$ Hz, 1H), 6.21 (s, 1H), 4.30 (br s, 2H), 4.08 (t, $J = 6.0$ Hz, 2H), 3.90 (br s, 2H), 3.40 (t, $J = 7.1$ Hz, 2H), 2.01 – 1.86 (m, 4H), 1.79 – 1.64 (m, 6H). ¹³C NMR (151 MHz, CDCl₃) δ : 195.52, 162.21, 161.30, 156.01, 155.86, 135.63, 129.58, 128.83, 128.83, 128.40, 128.40, 127.97, 112.68, 112.46, 111.80, 101.67, 68.06, 52.93, 51.29, 36.61, 29.71, 28.22, 26.00, 25.56, 24.33. HRMS: calcd for C₂₅H₂₈NO₃S₂ [M + H]⁺ 454.1432, found 454.1470. HPLC purity, 99.22%.

5.2.12. *4-((4-oxo-1,2,3,4-tetrahydrocyclopenta[c]chromen-7-yl)oxy)butyl piperidine-1-carbodithioate (7l)*

Yield 81%; yellow solid; m.p. 85-87 °C; IR (KBr): $\nu = 2930, 2864, 1707, 1609, 1470, 1432, 1283, 1233, 1159, 1035, 859, 762$ cm⁻¹. ¹H NMR (600 MHz, DMSO) δ : 7.52 (d,

$J = 8.6$ Hz, 1H), 7.01 (d, $J = 2.4$ Hz, 1H), 6.95 (dd, $J = 8.6, 2.4$ Hz, 1H), 4.21 (br s, 2H), 4.10 (t, $J = 6.1$ Hz, 2H), 3.89 (br s, 2H), 3.32 (t, $J = 7.0$ Hz, 2H), 3.06 (t, $J = 7.3$ Hz, 2H), 2.74 (t, $J = 7.4$ Hz, 2H), 2.14 – 2.07 (m, 2H), 1.87 – 1.76 (m, 4H), 1.69 – 1.60 (m, 2H), 1.60 – 1.51 (m, 4H). ^{13}C NMR (151 MHz, DMSO) δ : 194.23, 161.58, 159.75, 157.10, 155.72, 126.83, 123.80, 112.96, 112.19, 101.61, 68.21, 52.28, 51.30, 36.30, 32.13, 30.49, 28.13, 28.13, 25.65, 24.04, 24.04, 22.53. HRMS: calcd for $\text{C}_{22}\text{H}_{28}\text{NO}_3\text{S}_2$ $[\text{M} + \text{H}]^+$ 418.1432, found 418.1465. HPLC purity, 98.96%.

5.2.13. *4-((6-oxo-7,8,9,10-tetrahydro-6H-benzo[c]chromen-3-yl)oxy)butyl piperidine-1-carbodithioate (7m)*

Yield 88%; white solid; m.p. 89-90 °C; IR (KBr): $\nu = 2931, 2857, 1709, 1618, 1512, 1429, 1293, 1230, 1156, 1036, 860, 752$ cm^{-1} . ^1H NMR (600 MHz, CDCl_3) δ : 7.44 (d, $J = 8.8$ Hz, 1H), 6.83 (dd, $J = 8.8, 2.5$ Hz, 1H), 6.78 (d, $J = 2.5$ Hz, 1H), 4.30 (br s, 2H), 4.04 (t, $J = 6.0$ Hz, 2H), 3.90 (br s, 2H), 3.40 (t, $J = 7.0$ Hz, 2H), 2.75 (t, $J = 5.2$ Hz, 2H), 2.56 (t, $J = 6.1$ Hz, 2H), 1.99 – 1.88 (m, 4H), 1.89 – 1.76 (m, 4H), 1.76 – 1.62 (m, 6H). ^{13}C NMR (151 MHz, CDCl_3) δ : 195.58, 162.23, 160.82, 153.51, 147.33, 124.09, 120.45, 113.71, 112.31, 101.20, 67.87, 52.89, 51.29, 36.67, 29.71, 28.29, 26.00, 25.56, 25.24, 24.33, 23.85, 21.72, 21.42. HRMS: calcd for $\text{C}_{23}\text{H}_{30}\text{NO}_3\text{S}_2$ $[\text{M} + \text{H}]^+$ 432.1589, found 432.1627. HPLC purity, 99.69%.

5.2.14. *4-((6-oxo-6,7,8,9,10,11-hexahydrocyclohepta[c]chromen-3-yl)oxy)butyl piperidine-1-carbodithioate (7n)*

Yield 89%; white solid; m.p. 93-94 °C; IR (KBr): $\nu = 2922, 2850, 1694, 1617, 1557, 1454, 1428, 1296, 1226, 1155, 1074, 859, 761$ cm^{-1} . ^1H NMR (600 MHz, CDCl_3) δ :

7.55 (d, $J = 8.9$ Hz, 1H), 6.83 (dd, $J = 8.9, 2.5$ Hz, 1H), 6.80 (d, $J = 2.5$ Hz, 1H), 4.29 (br s, 2H), 4.05 (t, $J = 6.0$ Hz, 2H), 3.90 (br s, 2H), 3.39 (t, $J = 7.0$ Hz, 2H), 2.91 (t, $J = 5.3$ Hz, 2H), 2.88 (t, $J = 5.4$ Hz, 2H), 2.00 – 1.84 (m, 6H), 1.76 – 1.56 (m, 10H). ^{13}C NMR (151 MHz, CDCl_3) δ : 194.54, 161.51, 160.14, 153.19, 152.97, 124.22, 123.93, 112.36, 111.39, 100.39, 66.89, 51.88, 50.26, 31.06, 28.68, 27.24, 27.20, 25.64, 24.97, 24.87, 24.53, 24.16, 24.16, 23.31. HRMS: calcd for $\text{C}_{24}\text{H}_{32}\text{NO}_3\text{S}_2$ $[\text{M} + \text{H}]^+$ 446.1745, found 446.1785. HPLC purity, 99.74%.

5.3. General procedure for the synthesis of final compounds **8a-n**.

Except that the starting material piperidine was replaced by different commercial available secondary amines, the procedure for preparing target compounds **8a-n** was the same as that for preparation of **7a-n** (Scheme 2).

5.3.1. 4-((3-chloro-4-methyl-2-oxo-2H-chromen-7-yl)oxy)butyl [1,4'-bipiperidine]-1'-carbodithioate (**8a**)

Yield 82%; white solid; m.p. 118-120 °C; IR (KBr): $\nu = 2930, 2852, 1734, 1600, 1470, 1432, 1292, 1257, 1207, 1147, 1077, 860, 761$ cm^{-1} . ^1H NMR (600 MHz, CDCl_3) δ : 7.53 (d, $J = 8.9$ Hz, 1H), 6.91 (dd, $J = 8.9, 2.5$ Hz, 1H), 6.82 (d, $J = 2.5$ Hz, 1H), 4.08 (t, $J = 6.0$ Hz, 2H), 3.40 (br s, 2H), 3.15 (br s, 2H), 2.72 (br s, 1H), 2.58 (br s, 6H), 2.56 (s, 3H), 2.09 – 1.85 (m, 6H), 1.73 – 1.55 (m, 6H), 1.55 – 1.37 (m, 2H). ^{13}C NMR (151 MHz, CDCl_3) δ : 196.11, 161.96, 157.48, 153.12, 148.01, 125.86, 117.70, 113.32, 113.23, 101.32, 68.08, 62.16, 50.98, 50.24, 50.24, 49.08, 36.78, 30.57, 29.71, 28.17, 28.17, 25.90, 25.50, 24.40, 16.19. HRMS: calcd for $\text{C}_{25}\text{H}_{34}\text{ClN}_2\text{O}_3\text{S}_2$ $[\text{M} + \text{H}]^+$ 509.1621, found 509.1685. HPLC purity, 98.78%.

5.3.2. *4-((3-chloro-4-methyl-2-oxo-2H-chromen-7-yl)oxy)butyl*

4-phenylpiperidine-1-carbodithioate (8b)

Yield 86%; white solid; m.p. 155-156 °C; IR (KBr): $\nu = 2935, 2850, 1716, 1600, 1450, 1380, 1281, 1243, 1209, 1155, 1043, 862, 770 \text{ cm}^{-1}$. $^1\text{H NMR}$ (600 MHz, CDCl_3) δ : 7.51 (d, $J = 8.9 \text{ Hz}$, 1H), 7.46 – 7.29 (m, 3H), 7.25 – 7.15 (m, 2H), 6.90 (dd, $J = 8.9, 2.4 \text{ Hz}$, 1H), 6.81 (d, $J = 2.4 \text{ Hz}$, 1H), 4.08 (t, $J = 5.8 \text{ Hz}$, 2H), 3.43 (br s, 2H), 3.28 (br s, 2H), 3.03 – 2.80 (m, 2H), 2.54 (s, 3H), 2.14 – 1.73 (m, 9H). $^{13}\text{C NMR}$ (151 MHz, CDCl_3) δ : 196.06, 161.93, 157.44, 153.09, 147.98, 144.35, 128.64, 128.64, 126.72, 126.72, 126.69, 125.84, 117.68, 113.29, 113.20, 101.30, 68.08, 52.31, 50.64, 42.61, 36.71, 33.29, 32.72, 28.20, 25.52, 16.17. HRMS: calcd for $\text{C}_{26}\text{H}_{29}\text{ClNO}_3\text{S}_2$ [$\text{M} + \text{H}$] $^+$ 502.1199, found 502.1134. HPLC purity, 95.04%.

5.3.3. *4-((3-chloro-4-methyl-2-oxo-2H-chromen-7-yl)oxy)butyl*

4-hydroxypiperidine-1-carbodithioate (8c)

Yield 81%; white solid; m.p. 121-123 °C; IR (KBr): $\nu = 3528, 2947, 2919, 1721, 1598, 1476, 1432, 1290, 1258, 1210, 1140, 1081, 859, 761 \text{ cm}^{-1}$. $^1\text{H NMR}$ (600 MHz, CDCl_3) δ : 7.52 (d, $J = 8.9 \text{ Hz}$, 1H), 6.90 (dd, $J = 8.9, 2.5 \text{ Hz}$, 1H), 6.81 (d, $J = 2.5 \text{ Hz}$, 1H), 4.61 (br s, 1H), 4.19 (br s, 2H), 4.06 (t, $J = 6.1 \text{ Hz}$, 2H), 3.80 (br s, 1H), 3.40 (t, $J = 6.9 \text{ Hz}$, 2H), 2.55 (s, 3H), 2.01 – 1.89 (m, 6H), 1.77 – 1.60 (m, 4H). $^{13}\text{C NMR}$ (151 MHz, CDCl_3) δ : 196.10, 161.95, 157.53, 153.10, 148.06, 125.86, 117.69, 113.36, 113.23, 101.30, 68.08, 66.16, 48.38, 46.72, 36.78, 33.57, 29.71, 28.14, 25.48, 16.20. HRMS: calcd for $\text{C}_{20}\text{H}_{23}\text{ClNO}_4\text{S}_2$ [$\text{M} - \text{H}$] $^+$ 440.0835, found 440.0834. HPLC purity, 99.57%.

5.3.4. *4-((3-chloro-4-methyl-2-oxo-2H-chromen-7-yl)oxy)butyl**4-(hydroxymethyl)piperidine-1-carbodithioate (8d)*

Yield 85%; white solid; m.p. 84-86 °C; IR (KBr): $\nu = 3471, 2931, 2853, 1719, 1614, 1474, 1432, 1300, 1254, 1213, 1156, 1076, 863, 747 \text{ cm}^{-1}$. $^1\text{H NMR}$ (600 MHz, CDCl_3) δ : 7.51 (d, $J = 8.9 \text{ Hz}$, 1H), 6.89 (dd, $J = 8.9, 2.4 \text{ Hz}$, 1H), 6.80 (d, $J = 2.4 \text{ Hz}$, 1H), 4.67 (br s, 1H), 4.06 (t, $J = 6.0 \text{ Hz}$, 2H), 3.53 (br s, 2H), 3.39 (br s, 2H), 3.15 (br s, 2H), 2.54 (s, 3H), 2.00 – 1.78 (m, 7H), 1.57 (br s, 2H), 1.35 (br s, 2H). $^{13}\text{C NMR}$ (151 MHz, CDCl_3) δ : 195.93, 161.97, 157.54, 153.12, 148.06, 125.87, 117.70, 113.38, 113.23, 101.30, 68.10, 66.88, 51.65, 50.00, 38.55, 36.65, 28.72, 28.16, 28.16, 25.49, 16.20. HRMS: calcd for $\text{C}_{21}\text{H}_{27}\text{ClNO}_4\text{S}_2 [\text{M} + \text{H}]^+$ 456.0992, found 456.1077. HPLC purity, 98.50%.

5.3.5. *4-((3-chloro-4-methyl-2-oxo-2H-chromen-7-yl)oxy)butyl**4-methylpiperidine-1-carbodithioate (8e)*

Yield 82%; yellow solid; m.p. 81-83 °C; IR (KBr): $\nu = 2934, 2854, 1740, 1601, 1469, 1290, 1260, 1208, 1145, 1079, 866, 752 \text{ cm}^{-1}$. $^1\text{H NMR}$ (600 MHz, CDCl_3) δ : 7.51 (d, $J = 8.9 \text{ Hz}$, 1H), 6.90 (dd, $J = 8.9, 2.4 \text{ Hz}$, 1H), 6.81 (d, $J = 2.4 \text{ Hz}$, 1H), 4.07 (t, $J = 6.0 \text{ Hz}$, 2H), 3.40 (br s, 2H), 3.13 (br s, 2H), 2.55 (s, 3H), 2.03 – 1.85 (m, 4H), 1.81 – 1.62 (m, 4H), 1.25 (br s, 3H), 0.98 (d, $J = 6.1 \text{ Hz}$, 3H). $^{13}\text{C NMR}$ (151 MHz, CDCl_3) δ : 195.59, 168.95, 161.97, 157.49, 153.13, 147.99, 125.84, 117.71, 113.31, 113.22, 101.32, 68.10, 52.16, 50.42, 36.62, 34.02, 30.97, 28.19, 25.54, 21.28, 16.18. HRMS: calcd for $\text{C}_{21}\text{H}_{27}\text{ClNO}_3\text{S}_2 [\text{M} + \text{H}]^+$ 440.1043, found 440.1131. HPLC purity, 97.39%.

5.3.6. *4-((3-chloro-4-methyl-2-oxo-2H-chromen-7-yl)oxy)butyl**2-methylpiperidine-1-carbodithioate (8f)*

Yield 78%; yellow oli; IR (KBr): $\nu = 2937, 2867, 1739, 1600, 1502, 1479, 1294, 1259, 1205, 1145, 1078, 868, 753 \text{ cm}^{-1}$. $^1\text{H NMR}$ (600 MHz, CDCl_3) δ : 7.52 (d, $J = 8.9 \text{ Hz}$, 1H), 6.90 (dd, $J = 8.9, 2.3 \text{ Hz}$, 1H), 6.81 (d, $J = 2.3 \text{ Hz}$, 1H), 4.07 (t, $J = 5.9 \text{ Hz}$, 2H), 3.40 (t, $J = 7.0 \text{ Hz}$, 2H), 3.15 (br s, 1H), 2.55 (s, 3H), 2.07 – 1.87 (m, 4H), 1.86 – 1.46 (m, 8H), 1.27 (d, $J = 5.5 \text{ Hz}$, 3H). $^{13}\text{C NMR}$ (151 MHz, CDCl_3) δ : 195.85, 161.97, 157.48, 153.12, 147.99, 125.84, 117.70, 113.30, 113.21, 101.33, 68.11, 53.98, 46.37, 36.37, 30.09, 29.71, 28.23, 25.47, 25.47, 18.68, 16.18. HRMS: calcd for $\text{C}_{21}\text{H}_{27}\text{ClNO}_3\text{S}_2$ $[\text{M} + \text{H}]^+$ 440.1043, found 440.1134. HPLC purity, 95.68%.

5.3.7. *4-((3-chloro-4-methyl-2-oxo-2H-chromen-7-yl)oxy)butyl**-2,6-dimethylpiperidine-1-carbodithioate (8g)*

Yield 82%; yellow solid; m.p. 116-118 °C; IR (KBr): $\nu = 2942, 2869, 1731, 1602, 1509, 1467, 1296, 1233, 1204, 1153, 1079, 854, 752 \text{ cm}^{-1}$. $^1\text{H NMR}$ (600 MHz, CDCl_3) δ : 7.51 (d, $J = 8.9 \text{ Hz}$, 1H), 6.90 (dd, $J = 8.9, 2.5 \text{ Hz}$, 1H), 6.82 (d, $J = 2.5 \text{ Hz}$, 1H), 5.92 – 5.73 (m, 1H), 5.04 – 4.82 (m, 1H), 4.07 (t, $J = 5.6 \text{ Hz}$, 2H), 3.54 – 3.16 (m, 2H), 2.55 (s, 3H), 2.03 – 1.84 (m, 4H), 1.81 – 1.73 (m, 2H), 1.71 – 1.63 (m, 2H), 1.60 – 1.51 (m, 2H), 1.35 (d, $J = 7.0 \text{ Hz}$, 3H), 1.32 (d, $J = 7.0 \text{ Hz}$, 3H). $^{13}\text{C NMR}$ (151 MHz, CDCl_3) δ : 196.54, 161.97, 157.48, 153.12, 147.98, 125.83, 117.70, 113.30, 113.21, 101.33, 68.12, 53.63, 52.84, 36.37, 30.42, 30.16, 28.28, 25.33, 19.80, 18.71, 16.18, 13.98. HRMS: calcd for $\text{C}_{22}\text{H}_{28}\text{ClNO}_3\text{S}_2$ $[\text{M} + \text{Na}]^+$ 476.1199, found 476.1108. HPLC purity, 99.94%.

5.3.8. *4-((3-chloro-4-methyl-2-oxo-2H-chromen-7-yl)oxy)butyl dimethylcarbamodithioate (8h)*

Yield 87%; white solid; m.p. 127-129 °C; IR (KBr): $\nu = 2937, 1737, 1600, 1510, 1470, 1291, 1259, 1209, 1147, 1077, 863, 753 \text{ cm}^{-1}$. $^1\text{H NMR}$ (600 MHz, CDCl_3) δ : 7.52 (d, $J = 8.9 \text{ Hz}$, 1H), 6.90 (dd, $J = 8.9, 2.3 \text{ Hz}$, 1H), 6.81 (d, $J = 2.3 \text{ Hz}$, 1H), 4.07 (t, $J = 6.0 \text{ Hz}$, 2H), 3.56 (s, 3H), 3.44 – 3.33 (m, 5H), 2.55 (s, 3H), 2.07 – 1.82 (m, 4H). $^{13}\text{C NMR}$ (151 MHz, CDCl_3) δ : 197.12, 161.96, 157.49, 153.13, 147.99, 125.85, 117.72, 113.32, 113.23, 101.32, 68.09, 45.35, 41.47, 37.01, 28.14, 25.48, 16.18. HRMS: calcd for $\text{C}_{17}\text{H}_{21}\text{ClNO}_3\text{S}_2$ $[\text{M} + \text{H}]^+$ 386.0573, found 386.0671. HPLC purity, 99.40%.

5.3.9. *4-((3-chloro-4-methyl-2-oxo-2H-chromen-7-yl)oxy)butyl ethyl(methyl)carbamodithioate (8i)*

Yield 88%; white solid; m.p. 109-111 °C; IR (KBr): $\nu = 2938, 1743, 1601, 1471, 1283, 1260, 1209, 1147, 1079, 865, 752 \text{ cm}^{-1}$. $^1\text{H NMR}$ (600 MHz, CDCl_3) δ : 7.51 (d, $J = 8.9 \text{ Hz}$, 1H), 6.89 (dd, $J = 8.9, 2.5 \text{ Hz}$, 1H), 6.81 (d, $J = 2.5 \text{ Hz}$, 1H), 4.06 (t, $J = 6.0 \text{ Hz}$, 2H), 3.49 (br s, 2H), 3.37 (br s, 2H), 3.31 (br s, 2H), 2.54 (s, 3H), 2.00 – 1.85 (m, 5H), 1.25 (t, $J = 6.6 \text{ Hz}$, 3H). $^{13}\text{C NMR}$ (151 MHz, CDCl_3) δ : 195.32, 161.96, 157.51, 153.13, 147.99, 125.83, 117.73, 113.33, 113.23, 101.32, 68.09, 51.93, 31.93, 29.70, 28.17, 22.70, 16.18, 14.13. HRMS: calcd for $\text{C}_{18}\text{H}_{23}\text{ClNO}_3\text{S}_2$ $[\text{M} + \text{H}]^+$ 400.0730, found 400.0817. HPLC purity, 99.03%.

5.3.10. *4-((3-chloro-4-methyl-2-oxo-2H-chromen-7-yl)oxy)butyl diethylcarbamodithioate (8j)*

Yield 83%; white solid; m.p. 67-69 °C; IR (KBr): $\nu = 2943, 2869, 1737, 1601, 1508, 1480, 1287, 1260, 1209, 1143, 1078, 863, 754 \text{ cm}^{-1}$. ^1H NMR (600 MHz, CDCl_3) δ : 7.52 (d, $J = 8.8 \text{ Hz}$, 1H), 6.90 (dd, $J = 8.8, 1.8 \text{ Hz}$, 1H), 6.81 (d, $J = 1.8 \text{ Hz}$, 1H), 4.18 – 3.94 (m, 4H), 3.76 (br s, $J = 6.9 \text{ Hz}$, 2H), 3.38 (t, $J = 6.9 \text{ Hz}$, 2H), 2.55 (s, 3H), 2.05 – 1.75 (m, 4H), 1.29 (t, $J = 5.1 \text{ Hz}$, 6H). ^{13}C NMR (151 MHz, CDCl_3) δ : 195.47, 161.97, 157.50, 153.12, 148.00, 125.85, 117.70, 113.31, 113.22, 101.33, 68.10, 49.49, 46.70, 36.53, 28.20, 25.49, 16.18, 12.45, 11.61. HRMS: calcd for $\text{C}_{19}\text{H}_{25}\text{ClNO}_3\text{S}_2$ [$\text{M} + \text{H}$] $^+$ 414.0886, found 414.0981. HPLC purity, 95.41%.

5.3.11. *4-((3-chloro-4-methyl-2-oxo-2H-chromen-7-yl)oxy)butyl pyrrolidine-1-carbodithioate (8k)*

Yield 86%; white solid; m.p. 136-138 °C; IR (KBr): $\nu = 2939, 2854, 1730, 1599, 1507, 1471, 1284, 1249, 1203, 1123, 1074, 860, 753 \text{ cm}^{-1}$. ^1H NMR (600 MHz, CDCl_3) δ : 7.51 (d, $J = 8.9 \text{ Hz}$, 1H), 6.89 (dd, $J = 8.9, 2.4 \text{ Hz}$, 1H), 6.81 (d, $J = 2.4 \text{ Hz}$, 1H), 4.06 (t, $J = 6.0 \text{ Hz}$, 2H), 3.93 (t, $J = 6.9 \text{ Hz}$, 2H), 3.65 (t, $J = 6.9 \text{ Hz}$, 2H), 3.39 (t, $J = 7.0 \text{ Hz}$, 2H), 2.51 (s, 3H), 2.15 – 2.03 (m, 2H), 2.04 – 1.87 (m, 6H). ^{13}C NMR (151 MHz, CDCl_3) δ : 192.67, 161.97, 157.49, 153.13, 148.00, 125.84, 117.71, 113.32, 113.22, 101.33, 68.11, 55.01, 50.62, 35.85, 28.10, 26.04, 25.70, 24.29, 16.18. HRMS: calcd for $\text{C}_{19}\text{H}_{22}\text{ClNO}_3\text{S}_2$ [$\text{M} + \text{Na}$] $^+$ 434.0730, found 434.0841. HPLC purity, 97.63%.

5.3.12. *4-((3-chloro-4-methyl-2-oxo-2H-chromen-7-yl)oxy)butyl morpholine-4-carbodithioate (8l)*

Yield 81%; white solid; m.p. 132-134 °C; IR (KBr): $\nu = 2972, 2857, 1728, 1599, 1508, 1461, 1290, 1267, 1229, 1206, 1137, 1075, 867, 753 \text{ cm}^{-1}$. ^1H NMR (600 MHz,

CDCl₃) δ : 7.52 (d, J = 8.9 Hz, 1H), 6.90 (dd, J = 8.9, 2.2 Hz, 1H), 6.81 (d, J = 2.2 Hz, 1H), 4.35 (br s, 2H), 4.07 (t, J = 5.8 Hz, 2H), 3.98 (br s, 2H), 3.77 (br s, 4H), 3.42 (t, J = 7.0 Hz, 2H), 2.55 (s, 3H), 2.00 – 1.88 (m, 4H). ¹³C NMR (151 MHz, CDCl₃) δ : 197.51, 161.92, 157.47, 153.13, 147.98, 125.87, 117.76, 113.31, 113.26, 101.31, 68.04, 66.18, 66.18, 51.20, 50.38, 36.42, 28.18, 25.49, 16.19. HRMS: calcd for C₁₉H₂₃ClNO₄S₂ [M + H]⁺ 428.0986, found 428.0960. HPLC purity, 96.80%.

5.3.13. *4-((3-chloro-4-methyl-2-oxo-2H-chromen-7-yl)oxy)butyl*

4-methylpiperazine-1-carbodithioate (8m)

Yield 88%; white solid; m.p. 117-119 °C; IR (KBr): ν = 2965, 2938, 1738, 1602, 1465, 1287, 1259, 1226, 1206, 1141, 1077, 859, 761 cm⁻¹. ¹H NMR (600 MHz, CDCl₃) δ : 7.51 (d, J = 8.9 Hz, 1H), 6.89 (dd, J = 8.9, 2.5 Hz, 1H), 6.80 (d, J = 2.5 Hz, 1H), 4.39 (br s, 2H), 4.13 – 3.97 (m, 4H), 3.39 (t, J = 7.1 Hz, 2H), 2.56 (br s, 2H), 2.54 (br s, 5H), 2.38 (s, 3H), 2.05 – 1.68 (m, 4H). ¹³C NMR (151 MHz, CDCl₃) δ : 197.10, 161.93, 157.48, 153.12, 147.99, 125.86, 117.73, 113.31, 113.25, 101.31, 68.04, 54.25, 54.25, 50.63, 49.29, 45.40, 36.61, 28.17, 25.47, 16.18. HRMS: calcd for C₂₀H₂₆ClN₂O₃S₂ [M + H]⁺ 441.0995, found 441.1088. HPLC purity, 99.95%.

5.3.14. *4-((3-chloro-4-methyl-2-oxo-2H-chromen-7-yl)oxy)butyl*

4-isopropylpiperazine-1-carbodithioate (8n)

Yield 89%; white solid; m.p. 106-107 °C; IR (KBr): ν = 2963, 2871, 1734, 1601, 1511, 1469, 1291, 1257, 1229, 1206, 1148, 1078, 860, 761 cm⁻¹. ¹H NMR (600 MHz, CDCl₃) δ : 7.52 (d, J = 8.9 Hz, 1H), 6.90 (dd, J = 8.9, 2.4 Hz, 1H), 6.81 (d, J = 2.4 Hz, 1H), 4.39 (br s, 2H), 4.07 (t, J = 5.9 Hz, 2H), 4.00 (br s, 2H), 3.40 (t, J = 7.0 Hz, 2H),

2.80 (br s, 1H), 2.65 (br s, 4H), 2.55 (s, 3H), 2.04 – 1.84 (m, 4H), 1.13 – 0.74 (m, 6H).

^{13}C NMR (151 MHz, CDCl_3) δ : 196.59, 161.94, 157.47, 153.12, 147.99, 125.86, 117.73, 113.30, 113.24, 101.31, 68.06, 54.61, 51.11, 49.77, 48.09, 36.53, 29.70, 28.18, 25.51, 18.30, 18.30, 16.18. HRMS: calcd for $\text{C}_{22}\text{H}_{30}\text{ClN}_2\text{O}_3\text{S}_2$ $[\text{M} + \text{H}]^+$ 469.1308, found 469.1407. HPLC purity, 99.39%.

5.4 *In vitro* inhibition experiments of ChEs

The inhibition activities of designed compounds **7a-n** and **8a-n** against ChEs were determined according to Ellman's method [40]. Acetylcholinesterase (AChE, E.C. 3.1.1.7) from electric eel (eeAChE) and human erythrocytes (hAChE), butylcholinesterase (BuChE, E.C. 3.1.1.8) from equine serum (eqBuChE) and human serum (hBuChE), acetylthiocholine iodide (ATCI), S-butylthiocholine iodide (BTCI) and 5,5-dithiobis-(2-nitrobenzoic acid) (Ellman's reagent, DTNB) were purchased from Sigma-Aldrich (St. Louis, MO, USA). The target compound was dissolved in DMSO firstly and then diluted to different concentrations with Tris-HCl buffer solution (50 mM, pH = 8.0, 0.1 M NaCl, 0.02 M $\text{MgCl}_2 \cdot \text{H}_2\text{O}$) (DMSO < 0.01%). The experimental protocol was performed on 96-well plate. For each test well, 160 μL of DTNB (1.5 mM), 50 μL of AChE (0.22 U/mL eeAChE or 0.05 U/mL hAChE) or 50 μL of BuChE (0.12 U/mL eqBuChE or 0.024 U/mL hBuChE) and 10 μL of corresponding concentration of tested compound were added, and then the mixture was incubated at 37 °C for 6 min. After that, 30 μL of ATCI (15 mM) or BTCI (15 mM) as substrate was quickly added and the absorbance was determined with a wavelength of 405 nm by a UV plate reader (SpectraMax Plus 384, Molecular

Devices, Sunnyvale, CA, USA) at different time intervals (0, 60, 120, and 180 s). The inhibition activity of tested compound was reported with IC₅₀ value that was calculated as concentration of the compound that produced 50% enzyme activity inhibition. The results were expressed as mean \pm SD of three independent experiments. Data analysis was performed using Graph Pad Prism 4.03 software (San Diego, CA, USA).

5.5 In vitro inhibition experiments of MAOs.

The inhibition activities of compounds **7a-n** and **8a-n** towards MAOs were assayed by a fluorescence based method according to the experimental protocol previously reported[41; 42]. Recombinant human MAOs (hMAO-A and hMAO-B) and Amplex Red assay kit used to determine the production of H₂O₂ from substrate *p*-tyramine were purchased from Sigma-Aldrich (St. Louis, MO, USA) and Molecular Probes, Inc. (Eugene, Oregon, USA), respectively. Briefly, the test compound was dissolved in DMSO and then diluted to different concentrations with PBS buffer solution (DMSO < 0.01%). A mixture of inhibitor dilution and hMAO-A or hMAO-B was incubated at 37 °C for 15 min in test well of 96-well black microtiter plate. After this period, a substrate mixture from Amplex Red assay kit was added and a continuous fluorescence intensity (0-20 min) was determined at excitation/emission wavelengths of 545/590 nm. The IC₅₀ values of the test compounds were calculated using Graph Pad Prism 4.03 software. The results were expressed as mean \pm SD of three independent experiments.

5.6 In vitro blood-brain barrier permeation assay

The permeability of selected compounds for BBB was determined by a parallel artificial membrane permeation assay (PAMPA), which is a widely performed method established by Di et al [45]. Starting materials including the donor microplate (96-well filter plate, PVDF membrane, pore size is 0.45 μm), the acceptor microplate (indented 96-well plate) and 96-well UV plate (COSTAR) were purchased from Millipore and Corning Inc., respectively. Porcine brain lipid (PBL) and dodecane were acquired from Avanti Polar Lipids and Sigma-Aldrich, respectively. Commercial drugs were obtained from Aladdin Inc.. The test compound was dissolved in DMSO firstly and then diluted to corresponding concentration with a mixture of PBS/EtOH (70:30), which allowed the final concentration in each test well was 25 $\mu\text{g}/\text{mL}$. The artificial membrane of donor microplate was coated with 4 μL of PBL dissolved in dodecane (20 mg/mL). Then, 200 μL of diluted solution was added to each test donor well and 300 μL of PBS/EtOH (70:30) solution was added to corresponding acceptor well. The donor plate was carefully put on the acceptor plate to make the underside of filter membrane touch the buffer solution below. This sandwich formation was left undisturbedly for 18 h at 25 $^{\circ}\text{C}$. Afterwards, the donor plate was carefully removed, and the concentrations of tested compounds in acceptor and donor wells were determined separately by a UV plate reader (SpectraMax Plus 384, Molecular Devices, Sunnyvale, CA, USA). Each compound was determined at least three independent runs in four wells, and the results were expressed as mean \pm SD. P_e values of selected compounds and commercial drugs were calculated from the reported expression: $P_e = \{-V_d V_a / [(V_d + V_a) A t]\} \ln(1 - \text{drug}_{\text{acceptor}} / \text{drug}_{\text{equilibrium}})$, where V_d and V_a represents the

volume of donor well and acceptor well, respectively, A is the area of artificial membrane, t is the permeation time, drug acceptor is the absorbance assayed from the acceptor well, and drug equilibrium is the theoretical equilibrium absorbance. A good linear correlation between experimental P_e values of 9 standard drugs and their bibliographic values was obtained: P_e (exp.) = 0.9050 P_e (bibl.) - 0.2568 ($R^2 = 0.9759$).

5.7 Kinetic study of inhibition on AChE.

The kinetic study of AChE was performed by Ellman's method using hAChE [40]. Compound **8g** was dissolved in DMSO firstly and then diluted to the corresponding concentrations with Tris-HCl buffer solution (50 mM, pH = 8.0), which allowed the final concentrations in each test well were 37, 74 and 148 nM, respectively. The experiment was carried out on a 96-well plate. For each test well, 160 μ L of DTNB (1.5 mM), 50 μ L of hAChE (0.05 U/mL) and 10 μ L of diluted solution of compound **8g** were added, and then the mixture was incubated 6 min at 37 °C. After that, substrate in different concentrations (0.05–0.50 mM) was added to the corresponding well quickly and the absorbance was determined with a wavelength of 405 nm at different time intervals (0, 60, 120, and 180 s). Lineweaver–Burk reciprocal plots were established by plotting 1/velocity against 1/[substrate] at different concentrations of the substrate acetylthiocholine. The plots were assessed by a weighted least-squares analysis that assumed the variance of velocity (v) to be a constant percentage of v for the entire data set. Data analysis was performed using Graph Pad Prism 4.03 software (San Diego, CA, USA).

5.8. Reversibility and kinetic study of hMAO-B inhibition

The reversibility of compound **8g** towards MAO-B was determined by dilution assay[46]. Compound **8g** with concentrations equal to $10 \times IC_{50}$ and $100 \times IC_{50}$ for hMAO-B inhibition was treated with the enzyme (0.75 mg/mL) for 30 min at 37 °C in PBS (0.05 M, pH = 7.4). The parallel control was conducted by replacing the compound with buffer, and the corresponding amount of DMSO was added as co-solvent to all incubations. After the incubation period, the complex was diluted 100-fold to obtain final concentrations of compound **8g** equal to $0.1 \times IC_{50}$ and $0.1 \times IC_{50}$. For comparison, pargyline were incubated with hMAO-B at concentrations of $10 \times IC_{50}$ in similar manner and diluted to $0.1 \times IC_{50}$. The residual enzyme activity was determined by the method for the IC_{50} determination and all results were expressed as mean \pm SD.

The inhibition mechanism of hMAO-B by compound **8g** was investigated by construction of the Lineweaver–Burk reciprocal plots. Three concentrations (63, 126 and 252 nM) of compound **8g** were applied for kinetic study. The plots were established according to the initial catalytic rates of hMAO-B in the absence and in the presence of corresponding concentrations of inhibitor **8g** at six different concentrations (0.05, 0.1, 0.5, 1.0, 1.5, and 3.0 mM) of *p*-tyramine. The experimental conditions were similar to IC_{50} determination. The result data was analyzed using Graph Pad Prism 4.03 software (San Diego, CA, USA).

5.9 Molecular modeling studies

Docking simulations were performed using Molecular Operating Environment (MOE,

version 2008.10) software (Chemical Computing Group, Montreal, Canada). The crystal structures of human AChE (hAChE) in complex with donepezil (PDB code 4EY7) and human MAO-B in complex with 7-(3-chlorobenzoyloxy)-4-(methylamino)methyl-coumarin (PDB code 2V61) were obtained from the Protein Data Bank (PDB). The enzyme structures were firstly checked for missing atoms, bonds and contacts. Then, the hydrogens and partial charges were added using protonate 3D application in MOE. Compound **8g** was constructed using the MOE builder module and energy minimized using Merck Molecular force field (MMFF94x, RMSD gradient: $0.05 \text{ kal mol}^{-1} \text{ \AA}^{-1}$). After this, the compound was docked into the active sites of the proteins by the Triangle Matcher placement method. The Dock scoring in MOE software was done using ASE scoring function and Force field was selected as the refinement method. The best 10 poses of the compound were retained and scored. When the docking was completed, the retained best poses were visually inspected and the interactions with binding pocket residues were analyzed using the MOE's pose viewer.

5.10 SH-SY5Y neuroblastoma cell toxicity assay

Cytotoxicity investigation was performed by MTT assay according to the experimental protocol previously described[47]. Human neuroblastoma SH-SY5Y cells were grown in a 1:1 mixture of Eagle's minimum essential medium (EMEM) and ham's F-12 medium supplemented with 10% fetal bovine serum (FBS), 100 U/mL penicillin and 100 $\mu\text{g/mL}$ streptomycin in 5% CO_2 at 37 °C. SH-SY5Y cells were seeded into 96-well plates at a density of 10000 cells/well and then treated with

different concentrations of compound **8g** (6.25-100 μM) or donepezil for 24 h. After that, 20 μL of MTT was added and the mixture was incubated at 37 $^{\circ}\text{C}$ for 4 h. Then, the medium was removed and 200 μL of DMSO was added to dissolve the formazan crystal in test well. The absorbance of DMSO solution was determined at a wavelength of 570 nm and a reference wavelength of 630 nm. The results were expressed as percentage of viable cells and depicted in **Figure 8** using Graph Pad Prism 4.03 software (San Diego, CA, USA). All data was analyzed as the mean \pm SD from three independent experiments.

5.11. Acute toxicity assay

A total of 40 Kunming mice (18-22 g, half male and half female) were purchased from Hunan SJA Laboratory Animal Co., Ltd (eligibility certification No. SCXK [xiang] 2016-0002). All mice were maintained in a standard animal house where provided constant temperature of 23 ± 2 $^{\circ}\text{C}$, relative humidity of $55 \pm 5\%$ and 12 h light-dark cycle. Distilled water and sterilized food were provided for mice. The mice were randomly divided into four groups according to the trial dose of compound **8g** (n = 10 per group, five male and five female): control group (0.5% carboxymethyl cellulose sodium salt solution), high dose group (2500 mg/kg), medium dose group (1250 mg/kg) and low dose group (645 mg/kg). Compound **8g** was suspended in 0.5% carboxymethyl cellulose sodium (CMC-Na) salt solution and delivered to tested animals by oral administration. All groups were fasted overnight and allowed free access to water before experiment. After administration, animals were observed continuously for the first 4 h for any abnormal behavioral changes or deaths, then

intermittently for the next 24 h, and occasionally thereafter for 14 days for the onset of any delayed effects. All mice were sacrificed on the 14th day, and possible toxic damage on heart, liver and kidneys was examined macroscopically.

5.12. Step-down passive avoidance test

Kunming mice (male, 18-22 g) were purchased from Hunan SJA Laboratory Animal Co., Ltd (eligibility certification No. SCXK [xiang] 2016-0002). All animals were maintained in a standard animal house controlled at constant temperature of 23 ± 2 °C with a relative humidity of $55 \pm 5\%$ and a 12 h light/dark. Scopolamine was purchased from Suicheng Pharmaceutical Co. Ltd. (Zhengzhou, China). Donepezil hydrochloride was obtained from the Energy Chemical Co., Ltd (Shanghai, China). The step-down test was performed in the passive avoidance chamber with a steel grid floor, where an insulated platform was placed in bottom right corner of the chamber [49]. Two separate trials were performed for the tested mice: a training trial and a recall trial. For the training trial, each mouse was allowed to get familiar with the chamber for 5 min. Then the power was on and the mouse was placed on the platform. Once the mouse stepped down, it would receive an electric shock (24 V, 0.5 mA), which caused it to return to the platform. The mice were randomly divided into six groups (n = 6 per group). Compound **8g** was suspended in 0.5% CMC-Na salt solution and delivered to tested animals at three doses of 20 mg/kg, 10 mg/kg and 5mg/kg by oral administration. For the experiment, compound **8g** or Donepezil was delivered to mice 1 h before each training trial. After 30 min, scopolamine (3 mg/kg, i.p.) was delivered to the mice to induce memory impairment. After a 24 h interval,

the recall trial was carried out, and the mice were placed on the platform again. The latency to step down on the grid for the first time and the errors that resulted in a shock within 5 min were measured as the learning and memory performance.

Acknowledgement

This research work was financially supported by the Program of the National Natural Science Foundation of China [Grant No. 21807052, 81760622, 31600265]; the Program of Natural Science Foundation of Jiangxi Province of China [grant No. 20171BAB215064]; Research Fund for the Doctoral Program of Jiangxi University of Traditional Chinese Medicine [Grant No. 2015BS008]; Project from Health and Family planning Commission of Jiangxi province [Grant No. 2016A048, 20173013]; Guangxi Key Laboratory of Brain and Cognitive Neuroscience, Guilin Medical University [07010150001].

References:

- [1] R.M. Anderson, C. Hadjichrysanthou, S. Evans, M.M. Wong, Why do so many clinical trials of therapies for Alzheimer's disease fail? *Lancet*. 390 (2017) 2327-2329.
- [2] A. Wimo, L. Jonsson, J. Bond, M. Prince, B. Winblad, The worldwide economic impact of dementia 2010, *Alzheimers Dement*. 9 (2013) 1-11.e3.
- [3] R. Cacabelos, Have there been improvements in Alzheimer's disease drug discovery over the past 5 years? *Expert Opin. Drug Discov*. 13 (2018) 523-538.
- [4] J.W. Ashford, Treatment of Alzheimer's Disease: The Legacy of the Cholinergic Hypothesis, Neuroplasticity, and Future Directions, *J. Alzheimers Dis*. 47 (2015) 149-156.

- [5] J. Hardy, D. Allsop, Amyloid deposition as the central event in the aetiology of Alzheimer's disease, *Trends Pharmacol. Sci.* 12 (1991) 383-388.
- [6] I. Grundkeiqbal, K. Iqbal, Y.C. Tung, M. Quinlan, Wisniewski, H.M.B. L, Abnormal phosphorylation of the microtubule-associated protein tau (tau) in Alzheimer cytoskeletal pathology, *Proc. Natl. Acad. Sci. U. S. A.* 83 (1986) 4913-4917.
- [7] M. Rosini, E. Simoni, A. Milelli, A. Minarini, C. Melchiorre, Oxidative stress in Alzheimer's disease: are we connecting the dots? *J. Med. Chem.* 57 (2014) 2821-2831.
- [8] S. Ayton, P. Lei, A.I. Bush, Biometals and their therapeutic implications in Alzheimer's disease, *Neurotherapeutics.* 12 (2015) 109-120.
- [9] A. Cavalli, M.L. Bolognesi, A. Minarini, M. Rosini, V. Tumiatti, M. Recanatini, C. Melchiorre, Multi-target-directed ligands to combat neurodegenerative diseases, *J. Med. Chem.* 51 (2008) 347-372.
- [10] M.B. Youdim, J.J. Buccafusco, CNS Targets for multi-functional drugs in the treatment of Alzheimer's and Parkinson's diseases, *J. Neural. Transm.* 112 (2005) 519-537.
- [11] R. León, A. G. Garcia, J. Marco-Contelles, Recent advances in the multitarget-directed ligands approach for the treatment of Alzheimer's disease. *Med. Res. Rev.* 33 (2013) 139-189.
- [12] V.N. Talesa, Acetylcholinesterase in Alzheimer's disease, *Mech. Ageing Dev.* 122 (2001) 1961-1969.
- [13] D. Muñoz-Torrero, Acetylcholinesterase inhibitors as disease-modifying therapies for Alzheimer's disease, *Curr. Med. Chem.* 15 (2008) 2433-2455.

- [14] J.L. Sussman, M. Harel, F. Frolow, C. Oefner, A. Goldman, L. Toker, I. Silman, Atomic structure of acetylcholinesterase from *Torpedo californica*: a prototypic acetylcholine-binding protein, *Science*. 253 (1991) 872-879.
- [15] M. Harel, G.J. Kleywegt, R.B. Ravelli, I. Silman, J.L. Sussman, Crystal structure of an acetylcholinesterase-fasciculin complex: interaction of a three-fingered toxin from snake venom with its target, *Structure*. 3 (1995) 1355-1366.
- [16] N.C. Inestrosa, M.C. Dinamarca, A. Alvarez, Amyloid-cholinesterase interactions. Implications for Alzheimer's disease, *FEBS J*. 275 (2008) 625-632.
- [17] M. Bartolini, C. Bertucci, V. Cavrini, V. Andrisano, beta-Amyloid aggregation induced by human acetylcholinesterase: inhibition studies, *Biochem. Pharmacol.* 65 (2003) 407-416.
- [18] M. Rosini, E. Simoni, M. Bartolini, A. Cavalli, L. Ceccarini, N. Pascu, D.W. McClymont, A. Tarozzi, M.L. Bolognesi, A. Minarini, V. Tumiatti, V. Andrisano, I.R. Mellor, C. Melchiorre, Inhibition of acetylcholinesterase, beta-amyloid aggregation, and NMDA receptors in Alzheimer's disease: a promising direction for the multi-target-directed ligands gold rush, *J. Med. Chem.* 51 (2008) 4381-4384.
- [19] D.E. Edmondson, A. Mattevi, C. Binda, M. Li, F. Hubálek, Structure and mechanism of monoamine oxidase, *Curr. Med. Chem.* 11 (2004) 1983-1993.
- [20] P. Riederer, M.B. Youdim, Monoamine oxidase activity and monoamine metabolism in brains of parkinsonian patients treated with l-deprenyl, *J. Neurochem.* 46 (1986) 1359-1365.
- [21] J. Grimsby, N.C. Lan, R. Neve, K. Chen, J.C. Shih, Tissue Distribution of Human

Monoamine Oxidase A and B mRNA, *J. Neurochem.* 55 (1990) 1166-1169.

[22] S. Carradori, R. Silvestri, *New Frontiers in Selective Human MAO-B Inhibitors*, *J. Med. Chem.* 58 (2015) 6717-6732.

[23] S. Schedinweiss, M. Inoue, L. Hromadkova, Y. Teranishi, N.G. Yamamoto, B. Wiehager, N. Bogdanovic, B. Winblad, A. Sandebringmatton, S. Frykman, Monoamine oxidase B is elevated in Alzheimer disease neurons, is associated with γ -secretase and regulates neuronal amyloid β -peptide levels, *Alzheimers Res. Ther.* 9 (2017) 57.

[24] O.M. Bautista-Aguilera, A. Samadi, M. Chioua, K. Nikolic, S. Filipic, D. Agbaba, E. Soriano, L. de Andres, M.I. Rodriguez-Franco, S. Alcaro, R.R. Ramsay, F. Ortuso, M. Yanez, J. Marco-Contelles, N-Methyl-N-((1-methyl-5-(3-(1-(2-methylbenzyl)piperidin-4-yl)propoxy)-1H-indol-2-yl)methyl)prop-2-yn-1-amine, a new cholinesterase and monoamine oxidase dual inhibitor, *J. Med. Chem.* 57 (2014) 10455-10463.

[25] L. Pisani, R. Farina, M. Catto, R.M. Iacobazzi, O. Nicolotti, S. Cellamare, G.F. Mangiatordi, N. Denora, R. Soto-Otero, L. Siragusa, C.D. Altomare, A. Carotti, Exploring Basic Tail Modifications of Coumarin-Based Dual Acetylcholinesterase-Monoamine Oxidase B Inhibitors: Identification of Water-Soluble, Brain-Permeant Neuroprotective Multitarget Agents, *J. Med. Chem.* 59 (2016) 6791-6806.

[26] J. Joubert, G.B. Foka, B.P. Repsold, D.W. Oliver, E. Kapp, S.F. Malan, Synthesis and evaluation of 7-substituted coumarin derivatives as multimodal monoamine oxidase-B and cholinesterase inhibitors for the treatment of Alzheimer's disease, *Eur. J. Med. Chem.* 125 (2017) 853-864.

- [27] O. Weinreb, T. Amit, O. Bar-Am, M.B. Youdim, Ladostigil: a novel multimodal neuroprotective drug with cholinesterase and brain-selective monoamine oxidase inhibitory activities for Alzheimer's disease treatment, *Curr. Drug Targets*. 13 (2012) 483-494.
- [28] P. Anand, B. Singh, N. Singh, A review on coumarins as acetylcholinesterase inhibitors for Alzheimer's disease, *Bioorg. Med. Chem.* 20 (2012) 1175-1180.
- [29] L.G. de Souza, M.N. Renna, J.D. Figueroa-Villar, Coumarins as cholinesterase inhibitors: A review, *Chem. Biol. Interact.* 254 (2016) 11-23.
- [30] Q. Sun, D.Y. Peng, S.G. Yang, X.L. Zhu, W.C. Yang, G.F. Yang, Syntheses of coumarin-tacrine hybrids as dual-site acetylcholinesterase inhibitors and their activity against butylcholinesterase, A β aggregation, and beta-secretase, *Bioorg. Med. Chem.* 22 (2014) 4784-4791.
- [31] L. Pisani, R. Farina, O. Nicolotti, D. Gadaleta, R. Soto-Otero, M. Catto, M. Di Braccio, E. Mendez-Alvarez, A. Carotti, In silico design of novel 2H-chromen-2-one derivatives as potent and selective MAO-B inhibitors, *Eur. J. Med. Chem.* 89 (2015) 98-105.
- [32] I.E. Orhan, and H.O. Gulcan, Coumarins: Auspicious Cholinesterase Monoamine Oxidase Inhibitors, *Curr. Top Med. Chem.* 15 (2015) 1673-1682.
- [33] R. Farina, L. Pisani, M. Catto, O. Nicolotti, D. Gadaleta, N. Denora, R. Soto-Otero, E. Mendez-Alvarez, C.S. Passos, G. Muncipinto, C.D. Altomare, A. Nurisso, P.A. Carrupt, A. Carotti, Structure-Based Design and Optimization of Multitarget-Directed 2H-Chromen-2-one Derivatives as Potent Inhibitors of Monoamine Oxidase B and

Cholinesterases, *J. Med. Chem.* 58 (2015) 5561-5578.

[34] S.S. Xie, X. Wang, N. Jiang, W. Yu, K.D. Wang, J.S. Lan, Z.R. Li, L.Y. Kong, Multi-target tacrine-coumarin hybrids: cholinesterase and monoamine oxidase B inhibition properties against Alzheimer's disease, *Eur. J. Med. Chem.* 95 (2015) 153-165.

[35] S.S. Xie, J.S. Lan, X. Wang, Z.M. Wang, N. Jiang, F. Li, J.J. Wu, J. Wang, L.Y. Kong, Design, synthesis and biological evaluation of novel donepezil-coumarin hybrids as multi-target agents for the treatment of Alzheimer's disease, *Bioorg. Med. Chem.* 24 (2016) 1528-1539.

[36] N. Jiang, Q. Huang, J. Liu, N. Liang, Q. Li, Q. Li, S.S. Xie, Design, synthesis and biological evaluation of new coumarin-dithiocarbamate hybrids as multifunctional agents for the treatment of Alzheimer's disease, *Eur. J. Med. Chem.* 146 (2018) 287-298.

[37] B. Darses, I.N. Michaelides, F. Sladojevich, J.W. Ward, P.R. Rzepa, D.J. Dixon, Expedient Construction of the [7-5-5] All-Carbon Tricyclic Core of the Daphniphyllum Alkaloids Daphnilongeranin B and Daphniyunnine D, *Org. Lett.* 14 (2012) 1684-1687.

[38] M.I. El-Gamal, C.H. Oh, Synthesis, in vitro antiproliferative activity, and in silico studies of fused tricyclic coumarin sulfonate derivatives, *Eur. J. Med. Chem.* 84 (2014) 68-76.

[39] R.D. Li, H.L. Wang, Y.B. Li, Z.Q. Wang, X. Wang, Y.T. Wang, Z.M. Ge, R.T. Li, Discovery and optimization of novel dual dithiocarbamates as potent anticancer agents,

Eur J Med Chem. 93 (2015) 381-391.

[40] G.L. Ellman, K.D. Courtney, A.V. Jr, R.M. Featherstone, A new and rapid colorimetric determination of acetylcholinesterase activity, *Biochem Pharmacol.* 7 (1961) 88-95.

[41] M. Yanez, N. Fraiz, E. Cano, F. Orallo, Inhibitory effects of *cis*- and *trans*-resveratrol on noradrenaline and 5-hydroxytryptamine uptake and on monoamine oxidase activity, *Biochem. Biophys. Res. Commun.* 344 (2006) 688-695.

[42] M.J. Matos, C. Teran, Y. Perez-Castillo, E. Uriarte, L. Santana, D. Vina, Synthesis and study of a series of 3-aryl coumarins as potent and selective monoamine oxidase B inhibitors, *J. Med. Chem.* 54 (2011) 7127-7137.

[43] A.C. Tripathi, S. Upadhyay, S. Paliwal, S.K. Saraf, Privileged scaffolds as MAO inhibitors: Retrospect and prospects, *Eur. J. Med. Chem.* 145 (2018) 445-497.

[44] D. Secci, S. Carradori, A. Bolasco, P. Chimenti, M. Yanez, F. Ortuso, S. Alcaro, Synthesis and selective human monoamine oxidase inhibition of 3-carbonyl, 3-acyl, and 3-carboxyhydrazido coumarin derivatives, *Eur. J. Med. Chem.* 46 (2011) 4846-4852.

[45] L. Di, E.H. Kerns, K. Fan, O.J. McConnell, G.T. Carter, High throughput artificial membrane permeability assay for blood-brain barrier, *Eur. J. Med. Chem.* 38 (2003) 223-232.

[46] L.J. Legoabe, A. Petzer, J.P. Petzer, Selected C7-substituted chromone derivatives as monoamine oxidase inhibitors, *Bioorg. Chem.* 45 (2012) 1-11.

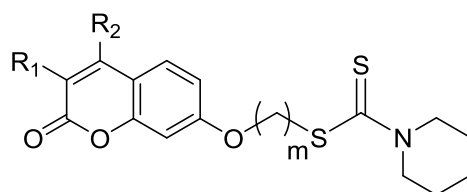
[47] X. Li, H. Wang, Z. Lu, X. Zheng, W. Ni, J. Zhu, Y. Fu, F. Lian, N. Zhang, J. Li, H.

Zhang, F. Mao, Development of Multifunctional Pyrimidinylthiourea Derivatives as Potential Anti-Alzheimer Agents, *J. Med. Chem.* 59 (2016) 8326-8344.

[48] C. Lu, Y. Guo, J. Yan, Z. Luo, H.B. Luo, M. Yan, L. Huang, X. Li, Design, synthesis, and evaluation of multitarget-directed resveratrol derivatives for the treatment of Alzheimer's disease, *J. Med. Chem.* 56 (2013) 5843-5859.

[49] I. Klinkenberg, A. Blokland, The validity of scopolamine as a pharmacological model for cognitive impairment: a review of animal behavioral studies, *Neurosci. Biobehav. Rev.* 34 (2010) 1307-1350.

[50] Z. Sang, W. Pan, K. Wang, Q. Ma, L. Yu, Y. Yang, P. Bai, C. Leng, Q. Xu, X. Li, Z. Tan, W. Liu, Design, synthesis and evaluation of novel ferulic acid-O-alkylamine derivatives as potential multifunctional agents for the treatment of Alzheimer's disease, *Eur. J. Med. Chem.* 130 (2017) 379-392.

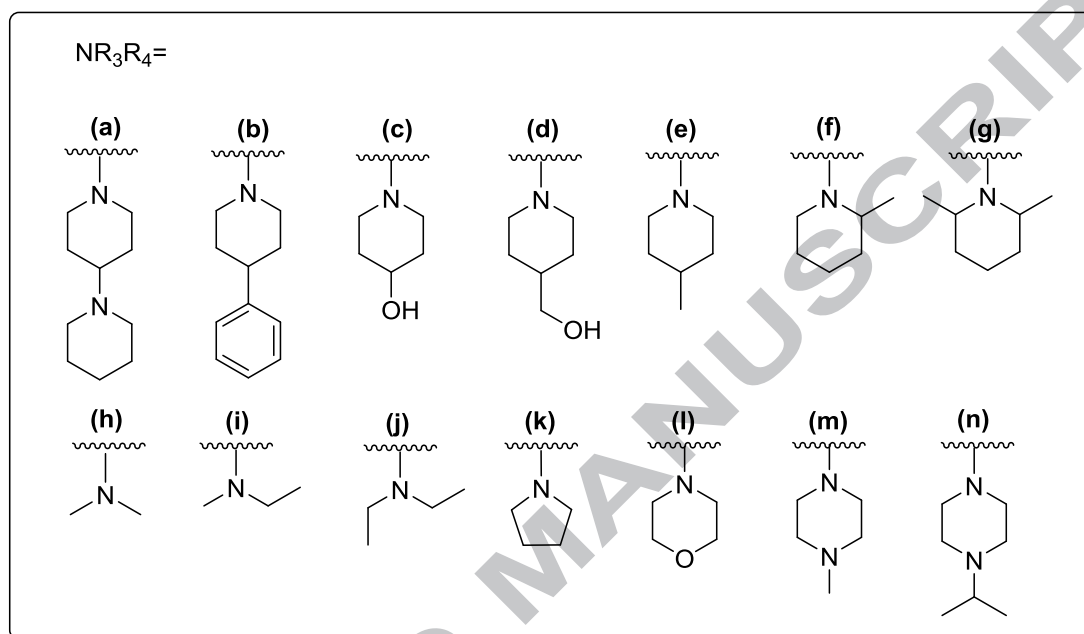
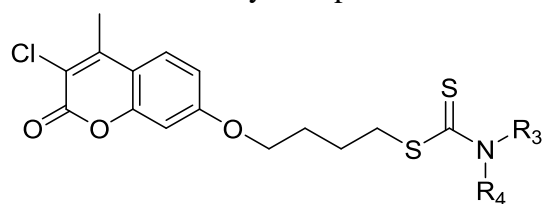
Table 1. Inhibition of ChEs and MAOs by Compounds **7a-n**.

Compd.	m	R ₁	R ₂	IC ₅₀ (μM) or inhibition (%) ^a			
				eeAChE ^b	eqBuchE ^c	hMAO-A ^d	hMAO-B ^e
7a	2	Me	Me	20.85 ± 1.04	17.13 ± 0.68%	n.a. ^f	17.19 ± 1.26
7b	3	Me	Me	1.39 ± 0.08	34.83 ± 1.81%	17.91 ± 0.70%	0.336 ± 0.012
7c	4	Me	Me	0.082 ± 0.003	31.20 ± 1.53%	5.94 ± 0.22%	0.662 ± 0.023
7d	5	Me	Me	0.088 ± 0.007	30.40 ± 1.88%	0.654 ± 0.021	0.251 ± 0.007
7e	4	H	H	0.218 ± 0.006	31.06 ± 1.13%	n.a. ^f	8.84 ± 0.46
7f	4	Me	H	0.367 ± 0.017	33.11 ± 1.35%	n.a. ^f	4.36 ± 0.15
7g	4	Cl	Me	0.061 ± 0.002	31.26 ± 1.19%	n.a. ^f	0.363 ± 0.009
7h	4	H	CF ₃	0.332 ± 0.009	23.69 ± 0.71%	n.a. ^f	42.12 ± 1.68
7i	4	COCH ₃	H	0.228 ± 0.005	30.53 ± 1.16%	10.44 ± 0.54%	12.29 ± 0.74
7j	4	COOEt	H	0.274 ± 0.014	28.47 ± 0.74%	n.a. ^f	39.0 ± 2.4
7k	4	H	Ph	15.48 ± 0.94	22.24 ± 0.68%	n.a. ^f	17.57 ± 0.67
7l	4	-(CH ₂) ₃ -		0.442 ± 0.024	20.12 ± 0.74%	n.a. ^f	4.0 ± 0.1
7m	4	-(CH ₂) ₄ -		0.229 ± 0.003	29.19 ± 1.28%	23.25 ± 0.94%	1.24 ± 0.04
7n	4	-(CH ₂) ₅ -		0.350 ± 0.011	22.52 ± 0.83%	n.a. ^f	21.40 ± 0.86

^a All values of IC₅₀ or inhibition % are shown as mean ± SD from three independent experiments.

^b From electric eel. ^c From equine serum. ^{d, e} Human MAO-B and MAO-A.

^f n. a. = no active. Compounds defined “no active” means that percent inhibition is less than 5.0% at a concentration of 50 μM in the assay conditions.

Table 2. Inhibition of ChEs and MAOs by Compounds **8a-n**.

Compd.	NR ₃ R ₄	IC ₅₀ (μM) or inhibition (%) ^a			
		eeAChE ^b	eqBuchE ^c	hMAO-A ^d	hMAO-B ^e
8a	a	9.64 ± 0.33	25.95 ± 1.14	n.a. ^f	7.47 ± 0.26
8b	b	18.46 ± 0.63	n.a. ^f	1.50 ± 0.06%	31.12 ± 1.21
8c	c	1.54 ± 0.05	21.75 ± 0.97%	12.69 ± 0.48%	5.60 ± 0.22
8d	d	4.75 ± 0.19	10.08 ± 0.29%	28.48 ± 1.16%	4.21 ± 0.18
8e	e	4.42 ± 0.13	29.81 ± 1.25%	29.70 ± 1.27%	0.347 ± 0.015
8f	f	0.0068 ± 0.0002	21.94 ± 1.01%	n.a. ^f	0.876 ± 0.036
8g	g	0.044 ± 0.002	23.28 ± 0.87%	5.85 ± 0.18	0.101 ± 0.024
8h	h	11.67 ± 0.51	20.85 ± 0.79%	11.15 ± 0.52%	2.07 ± 0.07
8i	i	0.217 ± 0.006	8.93 ± 0.41%	35.57 ± 1.62	7.49 ± 0.34
8j	j	0.167 ± 0.008	39.11 ± 1.80%	11.58 ± 0.69	0.788 ± 0.029
8k	k	0.386 ± 0.014	16.08 ± 0.64%	6.67 ± 0.29%	0.542 ± 0.027
8l	l	10.29 ± 0.39	11.86 ± 0.61%	n.a. ^f	47.16 ± 2.36
8m	m	4.57 ± 0.23	10.65 ± 0.49%	2.65 ± 0.07%	39.22 ± 1.80
8n	n	10.75 ± 0.48	33.09 ± 1.71%	2.09 ± 0.08	28.12 ± 1.15
donepezil		0.041 ± 0.001	4.22 ± 0.20	-	-
rasagiline		-	-	22.72 ± 1.43%	0.138 ± 0.004
iproniazid		-	-	6.52 ± 0.27	7.48 ± 0.34

^a All values are expressed as mean \pm SD from three independent experiments.

^b From electric eel. ^c From equine serum. ^{d,e} Human MAO-A and MAO-B.

^f n. a. = no active. Compounds defined “no active” means that percent inhibition is less than 5.0% at a concentration of 10 μ M (BuChE) or 50 μ M (MAO-A) in the assay conditions.

ACCEPTED MANUSCRIPT

Table 3. Inhibition of human ChEs by selected compounds.

Compd	IC ₅₀ (μM) ^a	
	hAChE	hBucHE
7c	0.147 ± 0.003	n.a. ^b
7g	0.031 ± 0.001	n.a. ^b
8f	0.0089 ± 0.0004	n.a. ^b
8g	0.114 ± 0.003	n.a. ^b
8j	0.196 ± 0.007	n.a. ^b
8k	0.392 ± 0.015	n.a. ^b
donepezil	0.021 ± 0.001	2.24 ± 0.11

^a All values are expressed as mean ± SD from three independent experiments.

^b n. a. = no active. Compounds defined “no active” means that percent inhibition is less than 10.0% at a concentration of 10 μM (hBuChE) .

Table 4 Permeability P_e ($\times 10^6$ cm/s) in the PAMPA-BBB assay for 9 commercial drugs in the experiment validation.

Commercial drugs	Bibliography ^a	Experiment ^b
Testosterone	17.0	15.10 \pm 0.73
Estradiol	12.0	9.72 \pm 0.61
Progesterone	9.3	8.13 \pm 0.36
Chlorpromazine	6.5	7.34 \pm 0.24
Caffeine	1.3	0.74 \pm 0.03
Corticosterone	5.1	4.90 \pm 0.13
Hydrocortisone	1.9	0.39 \pm 0.02
Atenolol	0.8	0.09 \pm 0.01
Theophylline	0.1	0.15 \pm 0.02

^a Taken from Ref [45].

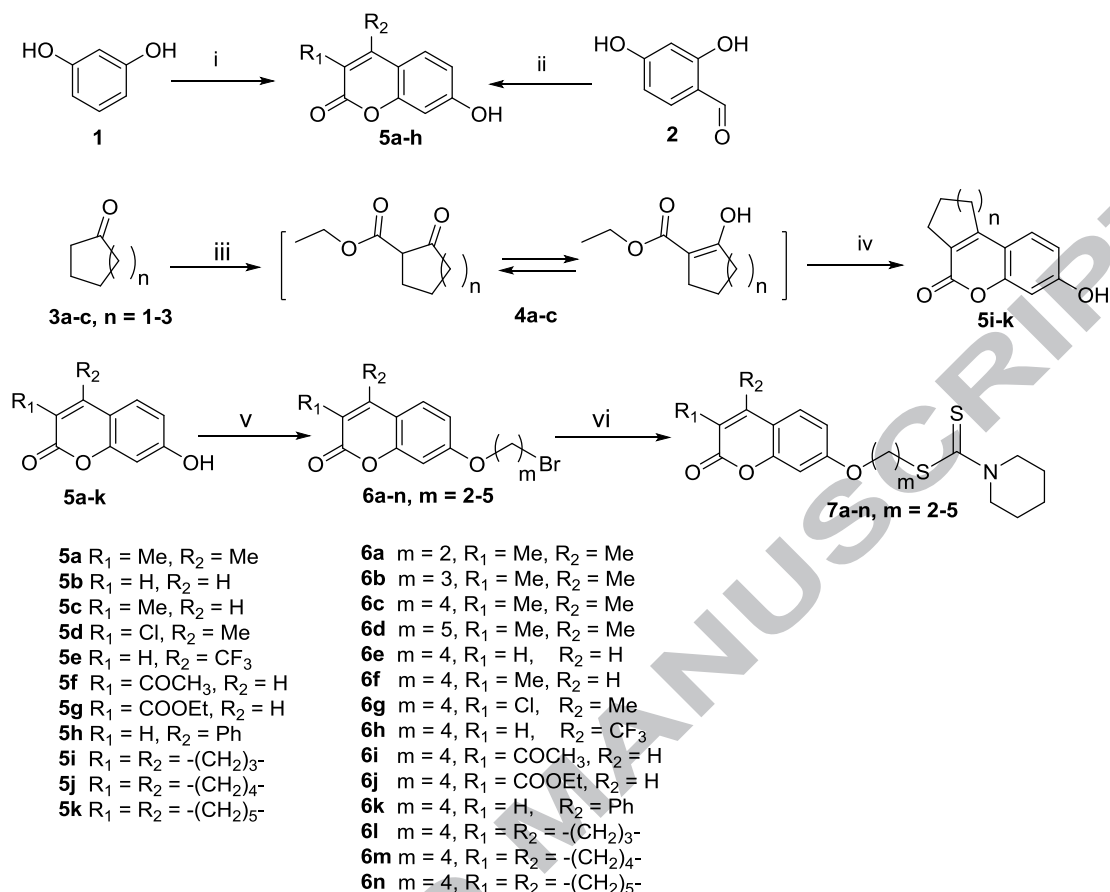
^b Experimental data are expressed as mean \pm SD from three independent experiments, using PBS : EtOH (70:30) as solvent.

Table 5 Permeability P_e ($\times 10^6$ cm/s) in the PAMPA-BBB assay for selected compounds and their predicted penetration into CNS.

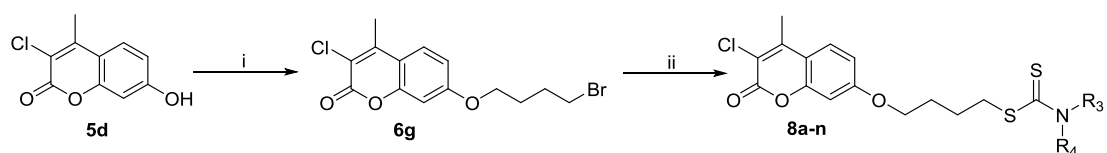
Compd.	P_e ($\times 10^6$ cm/s) ^a	Prediction ^b
7c	4.67 \pm 0.14	CNS+
7g	3.58 \pm 0.12	CNS+
8f	2.67 \pm 0.09	CNS \pm
8g	5.75 \pm 0.11	CNS+
8j	7.05 \pm 0.17	CNS+
8k	3.93 \pm 0.15	CNS+

^a Permeability P_e ($\times 10^6$ cm/s) values are expressed as mean \pm SD from three independent experiments, using PBS: EtOH (70:30) as solvent.

^b CNS + is predicted as high BBB permeation with P_e ($\times 10^6$ cm/s) $>$ 3.36, CNS \pm is uncertain for BBB permeation with $1.55 < P_e$ ($\times 10^6$ cm/s) $<$ 3.36.



Scheme 1. Synthesis of compounds **7a-n**. Reagents and conditions: (i) For **5a**, **5d** and **5h**: Ethyl 2-methylacetoacetate, ethyl 2-chloroacetoacetate or ethyl benzoylacacetate, conc. H_2SO_4 (cat.), 1,4-dioxane, 60 °C, 4 h; for **5b**: 2-Hydroxysuccinic acid, conc. H_2SO_4 (large excess), 100 °C, 2.5 h; for **5e**: Ethyl trifluoroacetoacetate, conc. H_2SO_4 (large excess), -40 °C to 0 °C, 1 h; (ii) Ethyl acetoacetate for **5f** and diethyl malonate for **5g**, piperidine, EtOH, reflux, 2 h; for **5c**: Sodium propionate, propionic anhydride, piperidine, reflux, 5 h; (iii) Diethyl carbonate, NaH, toluene, 100 °C, 2 h; (iv) Resorcinol, conc. H_2SO_4 , 0 °C; r.t., 4 h; (v) $\text{Br}(\text{CH}_2)_m\text{Br}$, anhydrous K_2CO_3 , acetone, reflux, 6 h; (vi) piperidine, TEA, CS_2 , DMF, r.t., 12 h.



Scheme 2. Synthesis of compounds **8a-n**. Reagents and conditions: (i) $\text{Br}(\text{CH}_2)_4\text{Br}$, anhydrous K_2CO_3 , acetone, reflux, 4 h, (ii) appropriate secondary amines, TEA, CS_2 , DMF, r.t., 12-24 h.

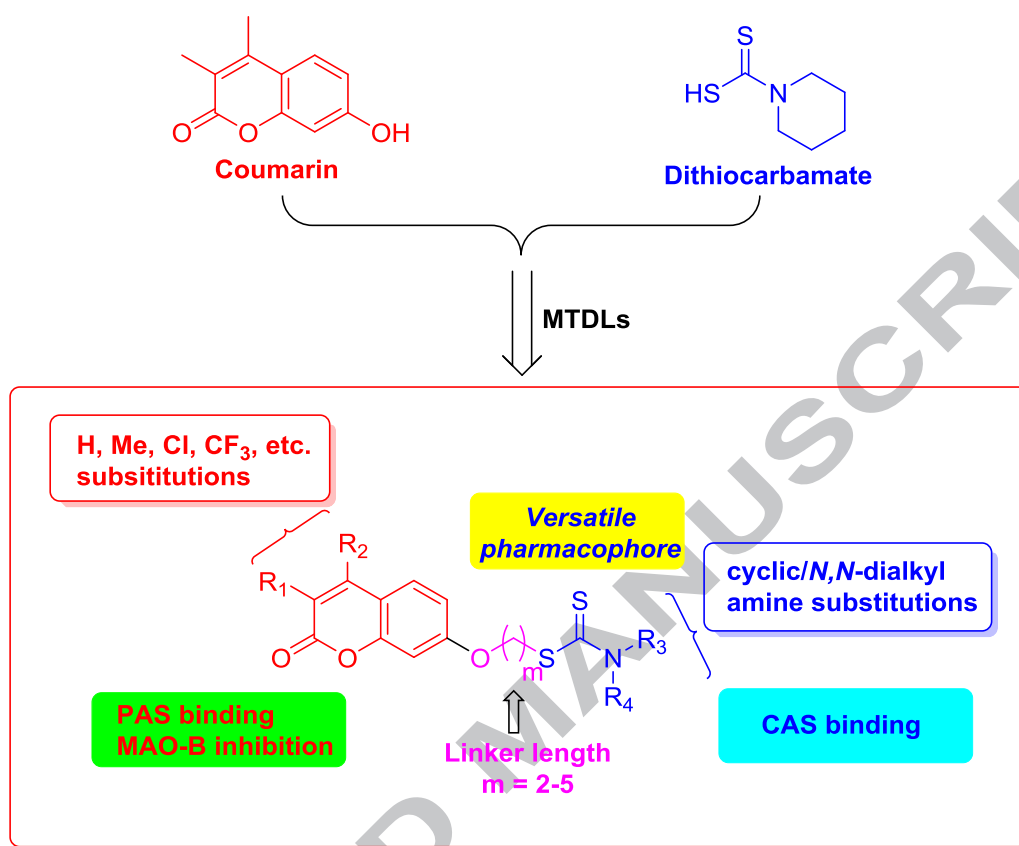


Figure 1. Design strategy for new coumarin-dithiocarbamate hybrids.

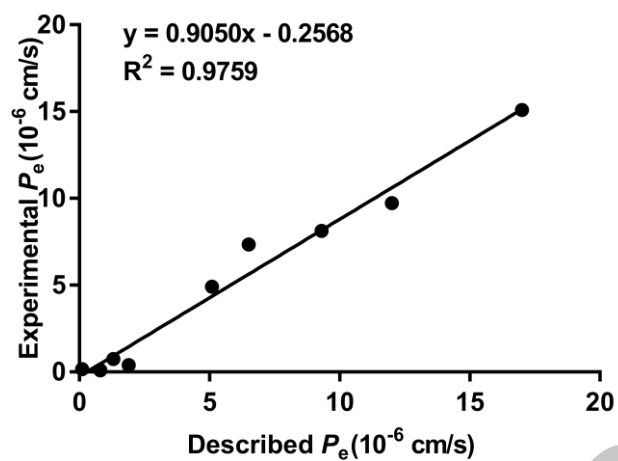


Figure 2. Lineal correlation between experimental and reported permeability of commercial drugs using the PAMPA-BBB assay. P_e (exp.) = $0.9050 P_e$ (bibl.) - 0.2568 ($R^2 = 0.9759$).

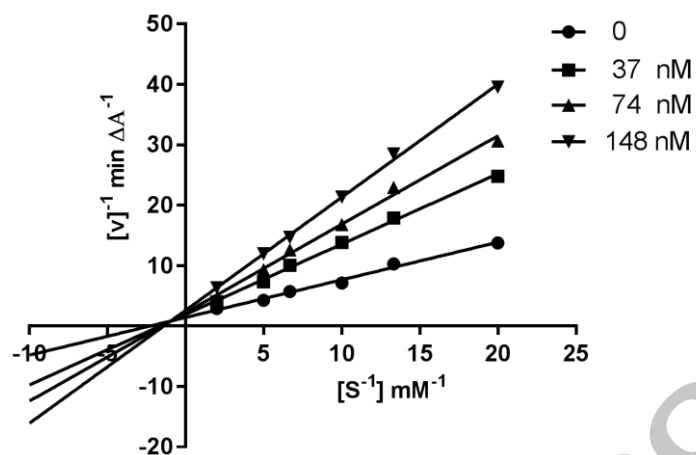


Figure 3. Kinetic study on the inhibition mechanism of hAChE by compound **8g**.

Overlaid Lineweaver–Burk reciprocal plots of hAChE initial velocity at increasing substrate concentrations (0.05–0.50 mM) in the absence of inhibitor and in the presence of different concentrations (37, 74 and 148 nM) of **8g** are shown.

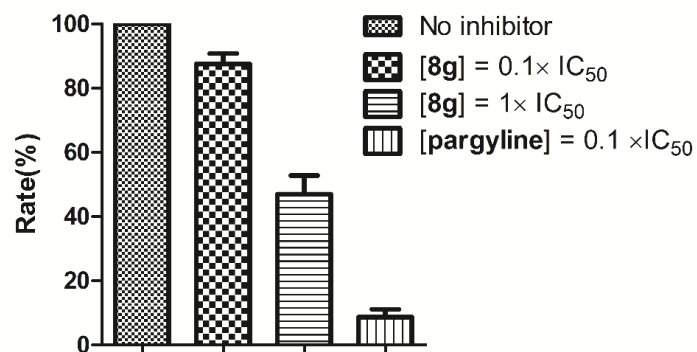


Figure 4. Recovery of enzyme activity after dilution of enzyme-compound complex.

Human MAO-B were pre-incubated with compound **8g** at concentrations equal to $10 \times IC_{50}$ and $100 \times IC_{50}$ for 30 min and then diluted to $0.1 \times IC_{50}$ and $1 \times IC_{50}$, respectively. The residual enzyme activities were subsequently measured.

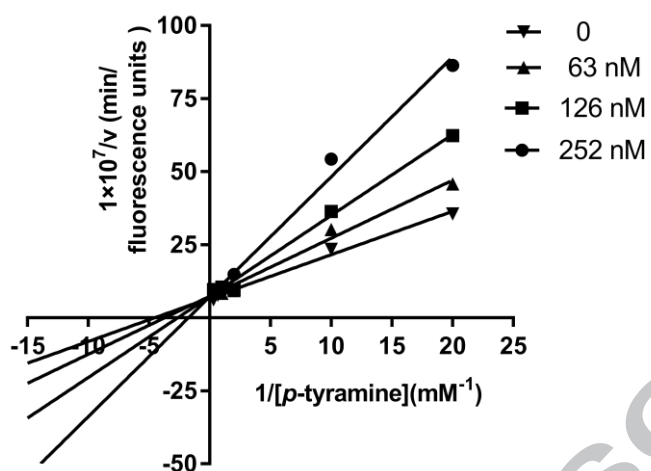


Figure 5. Kinetic study on the inhibition mechanism of hMAO-B by compound **8g**. Overlaid Lineweaver–Burk reciprocal plots of hMAO-B in the presence of different concentrations of **8g** (63, 126 and 252 nM) using *p*-tyramine (0.05–3.0 mM) as substrate are shown.

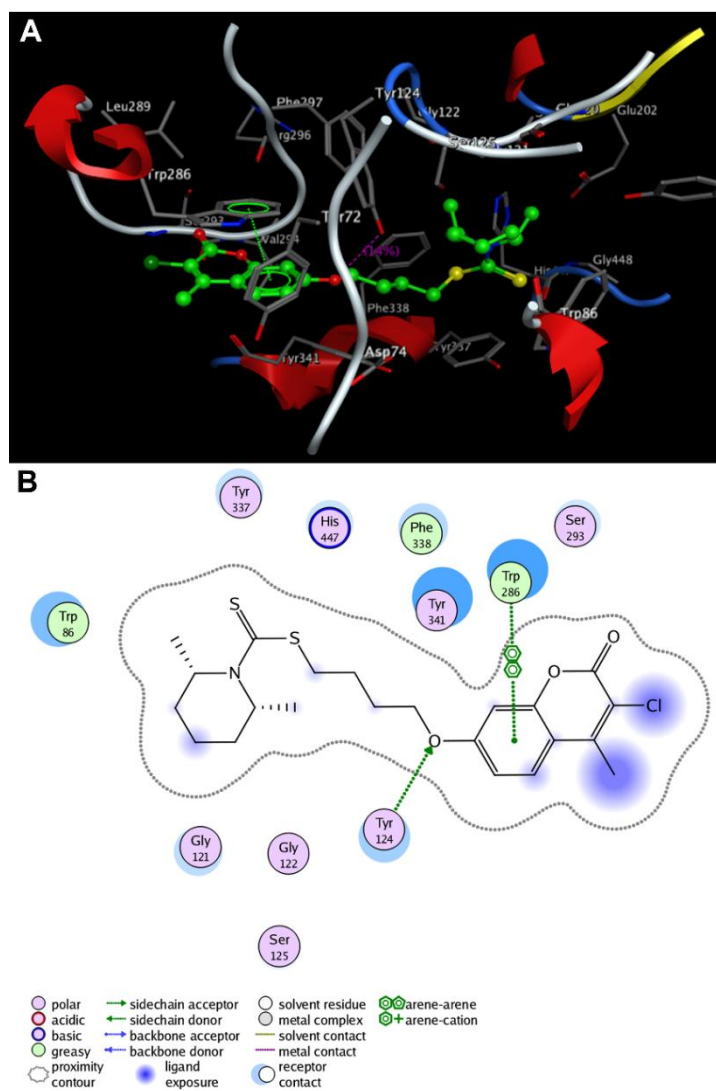


Figure 6. (A) 3D docking model of compound **8g** with hAChE. Atom colors: green-carbon atoms of **8g**, gray-carbon atoms of residues of hAChE, dark blue-nitrogen atoms, red-oxygen atoms, dark green-chlorine atoms, yellow-sulfur atoms. The dashed lines represent the interactions between the protein and the ligand. (B) 2D schematic diagram of docking model of compound **8g** with hAChE. The figure was prepared using the ligand interactions application in MOE.

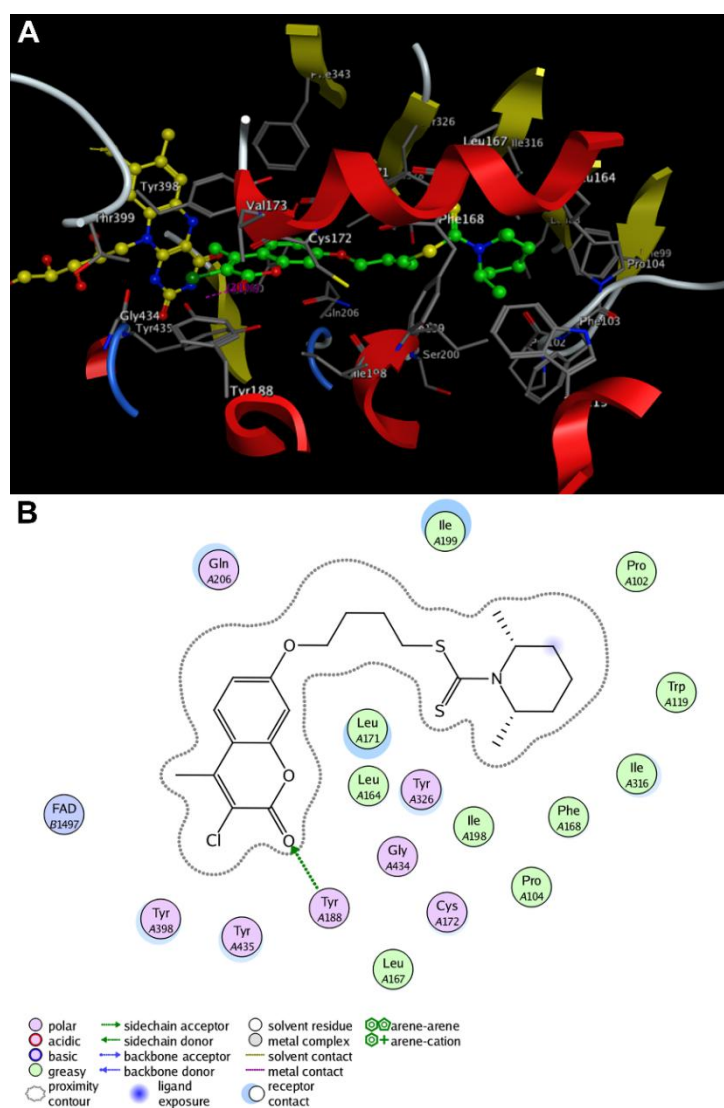


Figure 7. (A) 3D docking model of compound **8g** with hMAO-B. Atom colors: green-carbon atoms of **8g**, gray-carbon atoms of residues of hMAO-B, dark blue-nitrogen atoms, red-oxygen atoms, dark green-chlorine atoms, yellow-sulfur atoms. The dashed lines represent the interactions between the protein and the ligand. (B) 2D schematic diagram of docking model of compound **8g** with hMAO-B. The figure was prepared using the ligand interactions application in MOE.

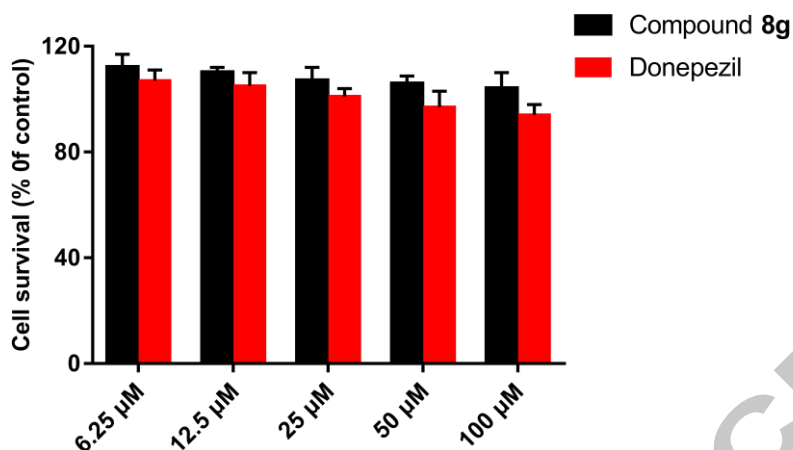


Figure 8. Cytotoxicity of compound **8g** and Donepezil on human neuroblastoma cells SH-SY5Y. SH-SY5Y cells were incubated with different concentrations of compound **8g** or Donepezil (6.25-100 μM) for 24 h. The results are shown as the percentage of viable cells after treatment with compound **8g** or Donepezil vs untreated control cells. Data are expressed as mean \pm SD from three independent experiments.

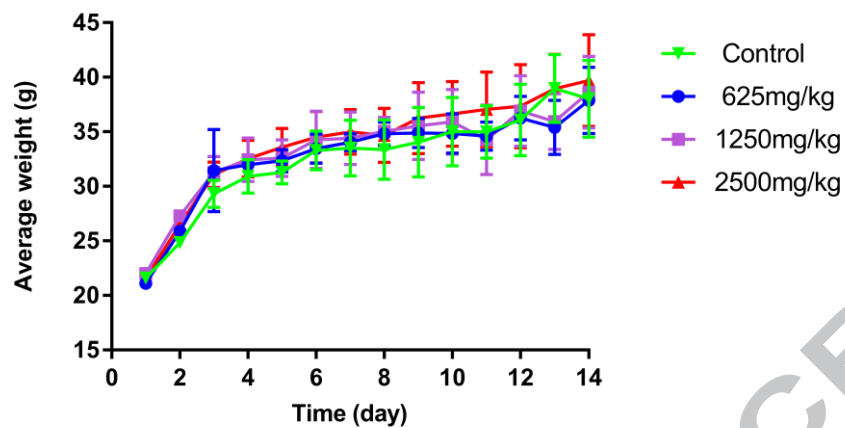


Figure 9. The effects on body weight of mice after oral administration of different concentrations of compound **8g**. Data are expressed as the average weight \pm SD of mice (n = 10).

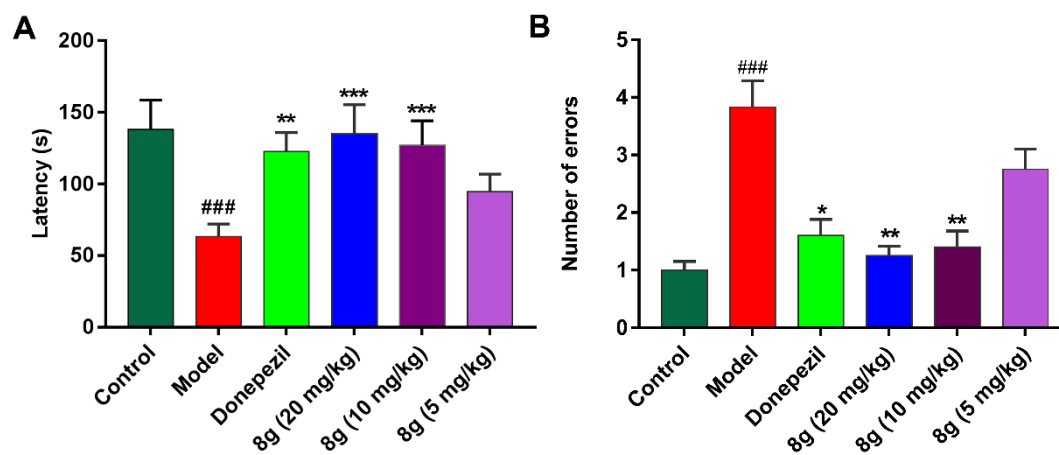


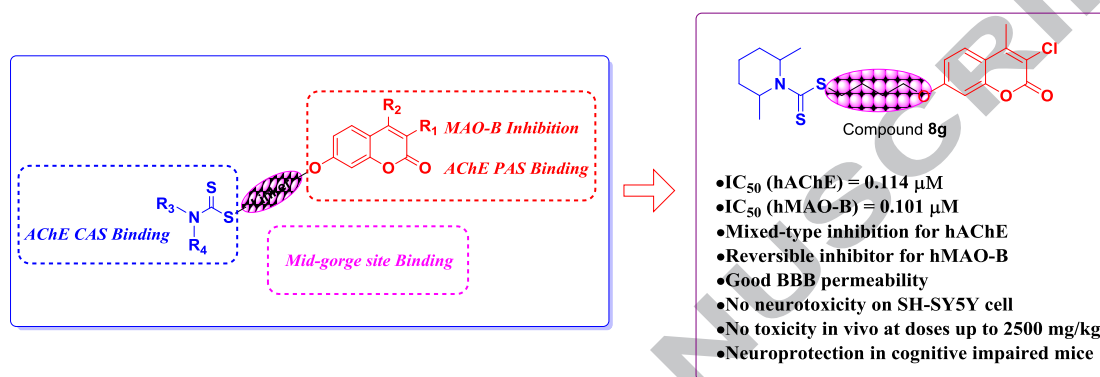
Figure 10. Effects of compound **8g** on the latency (**A**) and number of errors (**B**) in the step-down test by the scopolamine-induced cognitive impairment. The data are expressed as mean \pm SEM ($n = 6$). ### $P < 0.001$ vs. control group, * $P < 0.05$, ** $P < 0.01$, *** $P < 0.001$ vs. model group.

Graphical Abstract

Coumarin- dithiocarbamate hybrids as novel multitarget AChE and MAO-B

inhibitors against Alzheimer's Disease: Design, synthesis and biological

evaluation



Highlights

- Twenty-eight coumarin-dithiocarbamate hybrids were designed and synthesized.
- **8g** was identified as a potent and balanced inhibitor for AChE and MAO-B.
- **8g** showed no acute toxicity in mice and could penetrate the BBB.
- **8g** could significantly reverse scopolamine-induced memory deficit in vivo.